




Systematic review of *Atractus schach* (Serpentes: Dipsadidae) species complex from the Guiana Shield with description of three new species

Paulo Roberto Melo-Sampaio, Paulo Passos, Antoine Fouquet, Ana Lucia Da Costa Prudente & Omar Torres-Carvajal


To cite this article: Paulo Roberto Melo-Sampaio, Paulo Passos, Antoine Fouquet, Ana Lucia Da Costa Prudente & Omar Torres-Carvajal (2019) Systematic review of *Atractus schach* (Serpentes: Dipsadidae) species complex from the Guiana Shield with description of three new species, Systematics and Biodiversity, 17:3, 207-229, DOI: [10.1080/14772000.2019.1611674](https://doi.org/10.1080/14772000.2019.1611674)

To link to this article: <https://doi.org/10.1080/14772000.2019.1611674>

 View supplementary material 

 Published online: 20 Jun 2019.

 Submit your article to this journal 

 Article views: 577

 View related articles 






 View Crossmark data 

 Citing articles: 2 View citing articles 

Research Article



Systematic review of *Atractus schach* (Serpentes: Dipsadidae) species complex from the Guiana Shield with description of three new species

PAULO ROBERTO MELO-SAMPAIO¹ , PAULO PASSOS¹ , ANTOINE FOUQUET² ,
ANA LUCIA DA COSTA PRUDENTE³ , & OMAR TORRES-CARVAJAL⁴ 

¹Departamento de Vertebrados, Museu Nacional, Universidade Federal do Rio de Janeiro, Quinta da Boa Vista, Rio de Janeiro, RJ, 20940-040, Brazil

²Laboratoire Evolution et Diversité Biologique (EDB), UMR5174, Bâtiment 4R1, 118 Route de Narbonne, 31062 Toulouse cedex 9, France

³Laboratório de Herpetologia, Coordenação de Zoologia, Museu Paraense Emílio Goeldi, CP 399, Belém, Pará, 66040-170, Brazil

⁴Escuela de Biología, Pontificia Universidad Católica del Ecuador, Avenida 12 de Octubre y Roca, Apartado, Quito, 17-01-2184, Ecuador

(Received 8 August 2018; accepted 18 March 2019)

The Guiana Shield harbours one of the best preserved and largest extents of tropical forest on Earth and an immense biodiversity. The herpetofauna of this region remains poorly known. The species-rich snake genus *Atractus* contains ~140 species, many with complicated taxonomic histories, including *A. schach*. Examination of specimens in museums and newly collected material from French Guiana has allowed the illustration of hemipenial morphology for the first time and an expanded diagnosis. Concatenated molecular phylogenetic (mitochondrial and nuclear genes) and phenotypic (morphometrics, external and hemipenial morphology) analyses confirm non-monophyly of the *A. flammigerus* group and indicate that *A. schach* is a species complex with three new species described here. The geographic distribution of *A. schach sensu stricto* is restricted to Guiana, Surinam, and French Guiana north of Tumucumaque massif. Populations tentatively assigned to *A. schach* from the east from French Guiana in the Roura lowlands to Almeirim, and from central Amazonia between the Negro and Trombetas rivers in Brazil are also recognized as new species. Our results suggest that populations from south of the Amazon River are not conspecific with those from the Guiana Shield.

<http://www.zoobank.org/urn:lsid:zoobank.org:pub:A7AE40BC-4716-4302-B3BE-1F43600B0A72>

Key words: Amazonia, Dipsadinae, endemism, hemipenial morphology, molecular phylogeny, snakes, taxonomy

Introduction

The Guiana Shield (GS hereafter) is a Precambrian geological formation found in the north-east of South America (Hammond, 2005). The GS harbours one of the best preserved and greatest extents of tropical forest on Earth and an immense biodiversity (Hoogmoed, 1979; Hollowell & Reynolds, 2005). The herpetofauna of this region remains poorly known (Ávila-Pires, 2005; Fouquet, Gilles, Vences, & Marty, 2007; Fouquet et al., 2018; Vacher et al., 2017) though many recent works have improved the taxonomy of several herpetological groups, such as snakes (Passos, Kok, Albuquerque, &

Rivas, 2013). Although efforts have been made to understand patterns of occurrence and distribution of species across the GS, we have a limited knowledge of current richness and endemism, which are expected to be substantially underestimated (Fouquet et al., 2007; Funk, Caminer, & Ron, 2012; Vacher et al., 2017).

Many snakes from Neotropical highlands are putatively narrowly endemic (Fraga et al., 2017; Moraes et al., 2017). By contrast, most Amazonian lowland species have been considered to have widespread distributions (e.g., Almeida, Feitosa, Passos, & Prudente, 2014; Passos & Prudente, 2012). However, many recent discoveries, notably in taxa with a secretive lifestyle (fossorial or cryptozoic), have challenged this view revealing many cryptic lowland species with narrow

Correspondence to: Paulo Roberto Melo-Sampaio. E-mail: pmelosampaio@gmail.com

spatial ranges (Hoogmoed, Pinto, Rocha, & Pereira, 2009; Ribeiro, Silva, & Lima, 2016). Consequently, the taxonomy of some groups with wide distribution across Amazonia remains in a state of flux (Kok, 2010; Murphy *et al.*, 2016; Passos, Kok, *et al.*, 2013; Prudente & Passos, 2008; Zaher, Oliveira, & Franco, 2008). With 6 million km², some areas within the Amazon forest remain poorly sampled. Therefore, the Amazonian fauna would benefit from greater systematic investigation through complementary approaches and inventories (Ávila-Pires, Hoogmoed, & Vitt, 2007; Ávila-Pires, Hoogmoed, & Rocha, 2010; Moraes *et al.*, 2017).

With 140 described species, the dipsadid snake *Atractus* is the most speciose genus of living snakes (Passos, Teixeira, *et al.*, 2013). However, many of the currently recognized species are known exclusively from their type series, and aspects related to geographic, ontogenetic and/or sexual variability, as well as polychromatism, common in the genus, have not yet been properly evaluated (Passos, Cisneros-Heredia, Rivera, Aguilar, & Schargel, 2012). For these reasons, the taxonomic status of many taxa remains ambiguous (Passos, Fernandes, Bémils, & Moura-Leite, 2010). This is case notably for many *Atractus* from the GS because their original descriptions were brief or inaccurate, notably with the absence of specific provenance data and/or destination of the type material (Passos, Rivas & Barrio-Amorós, 2009).

Six species of *Atractus* are considered to occur in the GS lowlands: *Atractus badius* (Boie), *A. favae* (Filippi), *A. flammigerus* (Boie), *A. schach* (Boie), *A. torquatus* (Duméril, Bribon, & Duméril, 1854), and *A. zidoki* Gasc & Rodrigues. Boie (1827) described *Brachyorrhos badius*, *B. flammigerus*, and *B. schach* based on individuals whose provenance was wrongly assigned to Java (Hoogmoed, 1980). Wagler (1828) erected the genus *Atractus* designating *A. trilineatus* as type species. Two years later, Wagler (1830) proposed the synonymy of *Atractus* with *Brachyorrhos* Kuhl. Later, Schlegel (1837) synonymized *Brachyorrhos* with *Calamaria* H. Boie. Dumeril *et al.* (1854) described *Rabdosoma torquatum* based on Boie's material, transferring *Calamaria badia* to the genus *Rabdosoma* A.M.C. Duméril. Boulenger (1894) resurrected the genus *Atractus* and transferred to it all *Rabdosoma* species including *R. badius*, and proposed the synonymy of the genera *Adelphicos* Jan 1862, *Brachyorrhos* (in part), *Calamaria* (in part), and *Isoscelis* Günther with *Atractus*. Hoogmoed (1980) rediscovered the syntypes of *A. flammigerus*, *A. schach*, and *A. torquatus* removing the first two from the synonymy of *A. badius*, also diagnosing all of them (see Hoogmoed, 1980; Passos & Prudente, 2012; Passos *et al.*, 2017 for additional information with respect to the taxonomic status of

mentioned species). Cunha and Nascimento (1983, 1984, 1993) reported additional specimens, expanding the concept of *Atractus schach* to include specimens from the eastern part of the state of Pará and the western part of the state of Maranhão (south-east of the Amazonian delta), Brazil. Additionally, Nascimento, Ávila-Pires, and Cunha (1988) reported material of *A. schach* from the BR-429 road in the state of Rondônia, Brazil and Martins and Oliveira (1993) reported seven additional specimens of *A. schach* from Presidente Figueiredo, state of Amazonas, Brazil, expanding the distribution of the species to southern and central Amazonia. However, these records in Brazilian Amazonia have never been assessed through integrative taxonomy. Recently, Passos, Prudente, and Lynch (2016) proposed the *Atractus flammigerus* group to accommodate *Atractus atratus* Passos & Lynch, *A. flammigerus*, *A. fuliginosus* (Hallowell), *A. major* Boulenger, *A. punctiventris* Amaral, *A. schach*, *A. snethlageae* (Cunha & Nascimento, 1978), *A. tartarus* Passos, Prudente & Lynch and *A. univittatus* (Jan) based on overall similarities (mainly in hemipenial morphology). However, the monophyly of this group was not recovered (Oliveira & Hernández-Ruz, 2016). So, the aim of this study is to provide a more complete systematic assessment of the *A. schach* species complex, integrating distinct systems of characters (both genotypic and phenotypic) to better understand *Atractus* diversity, delimit cryptic species, and improve diagnoses of all recognized taxa. We here focus on the narrowly distributed taxa apparently endemic to the GS and highlight the species complex of non-closely related taxa, previously referred to as *A. schach*, along Amazonia.

Materials and methods

Coordinates of localities were acquired in the field or obtained from museum catalogues or reliable literature records. We refined, when possible, the provenance of records obtained from the literature or in museum databases without specific field coordinates using the software Google Earth Pro 7.1.2 Google Earth Pro (v7.1.2, Google Inc., Mountain View, CA). We follow the biogeographic regionalization of Morrone (2014) employed by Passos *et al.* (2016) to facilitate comparisons among species. This study is restricted to provinces 33 and 34 (Guianan Lowlands and Roraima provinces).

Molecular sampling, techniques, and selection of sequences

We obtained liver tissue samples of 53 individuals belonging to 11 nominal species: *Atractus badius*,

Table 1 Newly specimens sequenced in this work.

SPECIES	VOUCHER	16S	CMOS	CYTB	ND4	NT3	RAG 1
<i>Atractus badius</i>	AF1558	MH790471	MK835858	MK835884		MK835973	MK835943
<i>Atractus badius</i>	MNRJ 26710			MK835885			
<i>Atractus badius</i>	MNRJ 26711		MK835859	MK835886		MK835974	MK835944
<i>Atractus badius</i>	MNRJ 26712	MH790472	MK835860	MK835887		MK835975	MK835945
<i>Atractus badius</i>	MNRJ 26713	MH790473	MK835861			MK835976	MK835946
<i>Atractus badius</i>	MNRJ 26714	MH790474	MK835862	MK835888		MK835977	
<i>Atractus badius</i>	MNRJ 26715	MH790475	MK835863	MK835889		MK835978	MK835947
<i>Atractus badius</i>	MNRJ 26716			MK835890		MK835979	
<i>Atractus badius</i>	MNRJ 26717	MH790476	MK835864	MK835891		MK835980	MK835948
<i>Atractus badius</i>	MNRJ 26718	MH790477	MK835865	MK835892		MK835981	MK835949
<i>Atractus boimirim</i>	MPEG 21233	MH790478	MK835866			MK835982	
<i>Atractus dapsilis</i>	MNRJ 16794	MH790479		MK835893	MK835925		MK835950
<i>Atractus dapsilis</i>	MNRJ 16796	MH790480		MK835894	MK835926		MK835951
<i>Atractus dapsilis</i>	MNRJ 16802	MH790481		MK835895	MK835927		MK835952
<i>Atractus elaps</i>	QCAZ 5077						MK835953
<i>Atractus elaps</i>	QCAZ 5492					MK835985	
<i>Atractus elaps</i>	QCAZ 5574		MK835867	MK835896		MK835986	MK835954
<i>Atractus elaps</i>	QCAZ 7454		MK835868	MK835897		MK835987	
<i>Atractus elaps</i>	QCAZ 8217			MK835898		MK835988	MK835955
<i>Atractus elaps</i>	QCAZ 11581					MK835983	
<i>Atractus elaps</i>	QCAZ 14069					MK835984	
<i>Atractus flammigerus</i>	AF 1151	MH790483	MK835869	MK835899	MK835928	MK835989	
<i>Atractus flammigerus</i>	AF 3546	MH790484	MK835870	MK835900	MK835929	MK835990	
<i>Atractus flammigerus</i>	AF 3721	MH790485	MK835871	MK835901	MK835930	MK835991	
<i>Atractus flammigerus</i>	CAHE 9	MH790486	MK835872	MK835902		MK835992	
<i>Atractus flammigerus</i>	MNRJ 26719	MH790487			MK835931	MK835993	
<i>Atractus flammigerus</i>	MNRJ 26720	MH790488	MK835873	MK835903	MK835932	MK835994	
<i>Atractus latifrons</i>	CHUNB 47070	MH790490		MK835904			
<i>Atractus latifrons</i>	CHUNB 47071			MK835905			
<i>Atractus latifrons</i>	CHUNB 47134	MH790491		MK835906			
<i>Atractus latifrons</i>	CHUNB 47135	MH790492	MK835874	MK835907			
<i>Atractus latifrons</i>	MPEG 22630	MH790493	MK835875	MK835908			
<i>Atractus latifrons</i>	MPEG 24590			MK835909		MK835995	MK835956
<i>Atractus latifrons</i>	MTR 19392	MH790494	MK835876	MK835910		MK835996	MK835957
<i>Atractus major</i>	MNRJ 26126	MH790498		MK835911			MK835958
<i>Atractus major</i>	QCAZ 4691	MH790506		MK835912	MK835934	MK836002	
<i>Atractus major</i>	QCAZ 4993	MH790507			MK835935		
<i>Atractus major</i>	QCAZ 5891	MH790508	MK835877	MK835913	MK835936	MK836003	MK835962
<i>Atractus major</i>	QCAZ 7881	MH790509		MK835914	MK835937	MK836004	MK835963
<i>Atractus major</i>	QCAZ 8187	MH790510					
<i>Atractus major</i>	QCAZ 11565	MH790501	MK835878			MK835997	
<i>Atractus major</i>	QCAZ 11596	MH790502				MK835998	
<i>Atractus major</i>	QCAZ 11744	MH790503				MK835999	MK835959
<i>Atractus major</i>	QCAZ 13819	MH790504			MK835933	MK836000	MK835960
<i>Atractus major</i>	QCAZ 14321	MH790505				MK836001	MK835961
<i>Atractus major</i>	UFAC-RB 532	MH790511	MK835879	MK835915		MK836005	
<i>Atractus riveroi</i>	MNRJ 26087	MH790526		MK835916		MK836006	MK835964
<i>Atractus schach</i>	AF 1716	MH790527	MK835880	MK835917		MK836007	
<i>Atractus tartarus</i>	MPEG 23928	MH790528		MK835918			
<i>Atractus tartarus</i>	MPEG 23931	MH790529		MK835919	MK835938	MK836009	MK835965
<i>Atractus torquatus</i>	AF 2281	MH790530		MK835920	MK835939	MK836010	MK835966
<i>Atractus torquatus</i>	MPEG 21143	MH790531	MK835881		MK835940	MK836011	MK835967
<i>Atractus torquatus</i>	MPEG 23686	MH790532		MK835921	MK835941	MK836012	MK835968
<i>Atractus torquatus</i>	MTR 19069	MH790533		MK835922		MK836013	MK835969
<i>Atractus torquatus</i>	MTR 19408	MH790534	MK835882			MK836014	MK835970
<i>Atractus trefauti</i>	MNRJ 26709	MH790536	MK835883	MK835923	MK835942	MK836015	MK835971
<i>Atractus trilineatus</i>	MTR 20505			MK835924		MK836016	MK835972

A. boimirim Passos, Prudente & Lynch, *A. elaps* (Günther), *A. flammigerus*, *A. latifrons* (Günther), *A. major*, *A. riveroi* Roze *A. schach*, *A. tartarus*, *A.*

torquatus (Duméril, Bibron & Duméril, 1854), *A. trilineatus* Wagler, as well as four samples of two new species. Newly generated sequences are listed in Table 1.

Table 2. GenBank sequences used in this study.

Species	Voucher	12S	16S	CMOS	CYTB	ND4	NT3
<i>Atractus elaps</i>	DHMECN 10179		KY610052		KY610076	KY610101	
<i>Atractus elaps</i>	KU 214837				EF078536	EF078584	GU353273
<i>Atractus flammigerus</i>	MNHN 1997.2145	AF158402	AF158471				
<i>Atractus major</i>	DHMECN 8343		KY610059			KY610105	
<i>Atractus schach</i>	MNHN 1997.2371	AF158427	AF158486				
<i>Atractus</i> sp.	MPEG 21582	JQ598799	JQ598860	JQ598971			
<i>Atractus zidoki</i>	MNHN 1997.2046	AF158426	AF158487				
<i>Geophis godmani</i>	CAS 178126	JQ59881	JQ598877		JQ598932		

This material was obtained through both field sampling and loans from Museu Nacional, Universidade Federal do Rio de Janeiro (MNRJ), Museu Paraense Emílio Goeldi (MPEG) and Laboratory of Herpetology (MTR) at Universidade de São Paulo (USP), and Laboratoire Ecologie, Evolution, Interactions des Systèmes amazoniens (AF field number), at CNRS, Cayenne, French Guiana. Newly sequenced specimens are museum vouchers at the Museo de Zoología de la Pontificia Universidad Católica del Ecuador (QCAZ), Quito, Ecuador, Coleção Herpetológica da Universidade de Brasília (CHUNB), Brasília, Universidade Federal do Acre (UFAC-RB), Rio Branco and Museu Nacional, Universidade Federal do Rio de Janeiro (MNRJ), Rio de Janeiro, Brazil.

Genomic DNA was extracted under a guanidinium isothiocyanate extraction protocol (see details in Torres-Carvajal, Koch, Venegas, & Poe, 2017). Polymerase Chain Reaction (PCR) amplification of gene 16S, CYTB, C-MOS, NADH4, NT3, and RAG1 fragments were performed in a final volume of 24 μ L reactions using 1 \times PCR Buffer (–Mg), 3 mM MgCl₂, 0.2 mM dNTP mix, 0.2 μ M of each primer, 0.1 U/ μ L of Taq DNA Polymerase and 1.5 μ L of extracted DNA. Amplified products were treated with ExoSAP-IT (Affymetrix, Cleveland, OH) to remove remaining dNTPs and primers, and extraneous single-stranded DNA produced in the PCR. Double-stranded sequencing of PCR products was performed by Macrogen Inc. We amplified three mitochondrial and three nuclear gene fragments (primers in brackets): 16S [16Sar-L and 16Sbr-H-R (Palumbi *et al.*, 1991)], CYTB [LGL (Bickham, Wood, & Patton, 1995) and CytbV (Torres-Carvajal, Lobos, & Venegas, 2015)], NADH4 [ND413824H and ND412931L (Blair *et al.*, 2009)], and C-MOS [S77 and S78 (Lawson *et al.*, 2005)], NT3 [NT3-F3 e NT3-R4 (Kendall, Yeo, Henttu, & Tomlison, 2001)] and RAG1 [RAG1-MartF1 and RAG1-AmpR1 (Hoegg, Vences, Brinkmann, & Meyer, 2004)]. When available, we used GenBank sequences, limiting the sampling only to species known to occur in the GS. We examined all vouchers of sequences deposited in GenBank, except for two specimens: KU 214837

Atractus elaps from University of Kansas and BIOTA 1185 *A. tartarus* from Universidade Federal do Pará. We re-identified and excluded terminals for Atlantic species from previously published data (Grazziotin *et al.*, 2012). We excluded sequences with no vouchers, locality data, or both, and split the previously documented chimeras used by Pyron, Burbrink, and Wiens (2013) for *A. trihedrurus*, Pyron, Guayasamin, Peñafiel, Bustamante, and Arteaga (2015), Pyron, Arteaga, Echevarría, and Torres-Carvajal, (2016) and Figueroa, McKelvy, Grismer, Bell, and Lailvaux (2016) for *A. schach* and *A. zebrinus*. We excluded the sequences used by Arteaga *et al.* (2017) for *A. badius* and *A. major* (ANF 1545). All analysed sequence data were obtained from single voucher specimens to avoid 'chimeric sequence terminals'.

Sequence editing, alignment, and phylogenetic analyses

Data were assembled and aligned in Mega 7.0 (Kumar, Stecher, & Tamura, 2016) under default settings for Clustal W (Thompson, Higgins, & Gibson, 1994). Our dataset totalled 66 terminals, with 57 newly sequenced and nine from GenBank (Table 2). The concatenated matrix was built in SequenceMatrix (Vaidya, Lohman, & Meier, 2011). The best-fit nucleotide substitution models and partitioning scheme were determined simultaneously using PartitionFinder 2 (Lanfear, Frandsen, Wright, Senfeld, & Calcott, 2016), using the 'greedy' algorithm (Lanfear, Calcott, Ho, & Guindon, 2012), the 'MrBayes' set of models and the Bayesian information criterion to compare the fit of different models (Sullivan & Joyce, 2005). Genes were combined with seven partitions, one per non-coding gene and three per protein coding gene corresponding to each codon position. Bayesian inference was employed using MrBayes v3.2.1 (Ronquist *et al.*, 2012) on the CIPRES Science Gateway v3.3 (Miller, Pfeiffer, & Schwartz, 2010). All parameters except topology and branch lengths were unlinked between partitions. Four independent runs, each with four MCMC chains, were run for 20 million generations, sampling every 10,000 generations. We used

Tracer v1.6 (<http://beast.bio.ed.ac.uk/Tracer>) to assess convergence and stationarity by plotting the $-\ln L$ per generation, as well as to ensure effective sample sizes (ESS) >200 of model parameters. We combined runs using LogCombiner 1.8 after discarding 25% as burn-in and summarized sampled trees into a maximum clade credibility tree in TreeAnnotator v1.8.3 (Drummond, Suchard, Xie, & Rambaut, 2012). We chose *Geophis godmani* Boulenger, 1894 as outgroup following the rooting strategy of Arteaga et al. (2017). The phylogenetic tree was edited and visualized using FigTree v1.4.2 (<http://tree.bio.ed.ac.uk/software/figtree/>).

Terminology, techniques, characters, and presentation rationale

Terminology for cephalic shields follows Savage (1960) and Peters (1964) whereas ventral and subcaudal counts follow Dowling (1951). Condition of the loreal scale follows Passos, Fernandes, and Borges-Nojosa (2007). Measurements were taken with a Mitutoyo® digital calliper to the nearest 0.1 mm, except for snout–vent length (SVL) and tail length (TL), which were measured with a ruler to the nearest 1 mm. Measurements and descriptions of paired cephalic scales are strictly based on the left side of head. We follow the definition of Passos et al. (2016) for body marks (blotches, spots, and dots), where they counted separately for each side of the dorsum, and the use of ‘blotch’ refers to broader (two or more scales long and wide) dorsal marks located on the vertebral and paravertebral regions. Colour in preservative follows Köhler (2012). Sex determination was based on verification of the presence or absence of hemipenes through a ventral incision at the base of the tail.

We examined maxillae *in situ* under a Luxeo 4Z (Labomed) stereoscope through a narrow lateromedial incision between the supralabials and the maxillary arch. We counted teeth and empty sockets after removing tissues covering the maxillary bone. The method for preparation of preserved hemipenes was modified from Pesantes (1994) in replacing potassium hydroxide (KOH) with distilled water. Posteriorly, they were fully expanded with injection of coloured petroleum jelly (see Passos et al., 2016 for detailed explanation). Terminology for hemipenial descriptions follows Dowling & Savage (1960) and Zaher (1999) with a few minor adaptations following Passos et al. (Passos, Kok, et al., 2013; Passos et al., 2016). We follow Passos et al. (2010) regarding conditions of morphological characters used in diagnoses and descriptions. The species accounts are presented in chronological order with the specific subheadings synthesizing all

information for each character system according with Passos, Kok, et al. (2013). Institutional abbreviations follow Sabaj (2016), except for the field numbers. Data from additional specimens of *Atractus* examined from the GS are presented in Appendix I (see online supplemental material, which is available from the article’s Taylor & Francis Online page at <https://dx.doi.org/10.1080/14772000.2019.1614694>) to facilitate future comparisons and references, except those from Pantepui taxa and for *A. flammigerus* and *A. torquatus* listed in Passos et al. (Passos, Kok, et al., 2013; Passos et al., 2017) and Passos and Prudente (2012), respectively.

All the species recognized herein based on reciprocal monophyly (using molecular phylogenetics) exhibited unambiguous phenotypic diagnostic characters or exclusive combinations of traits observed in the morphological dataset. We used such characters to support the recognition of a given lineage in agreement with the recovered topology. Because most species from the GS and adjacent areas of Amazonia have not been included in previous molecular phylogenetic analyses, they have been placed tentatively in some species groups by previous authors (e.g., Passos et al., 2016), or have remained without group assignment (*A. riveroi* and *A. torquatus*).

Results

Phylogenetic analyses

We consider posterior probability values above 0.95 as strongly supported, values between 0.7 and 0.95 as moderately supported, and below 0.7 as weakly supported. The *Atractus flammigerus* group is not recovered as monophyletic (Fig. 1). *Atractus major* (with maximum support) and *A. boimirim* are successive sister taxa to a large clade containing all the other sampled species of *Atractus*. Within the next clade, *Atractus elaps* and *A. latifrons* form a strongly supported clade that is the sister group to remaining species, which are nested in two less well-supported subclades: (*A. badius*, (*A. torquatus*, (*A. riveroi*, *A. flammigerus*))) and ((*A. trilineatus*, *A. zidoki*), (*A. tartarus*, ((*A. dapsilis*, *A. sp.*), (*A. schach*, *A. trefauti*))))).

A small clade containing *A. trilineatus* and *A. zidoki* is recovered with low support (PP= 0.49). The latter species is a member of the *Atractus collaris* species group sharing several putative synapomorphies with *A. alphonsehogei*, *A. caxiuana*, *A. collaris*, *A. hoogmoedi*, and *A. surucucu* (Passos et al., 2013c; Passos, Prudente, Ramos, Caicedo-Portilla, & Lynch, 2018). *Atractus tartarus*, previously considered as a member of *A. flammigerus* group (Passos et al. 2016), is recovered as sister

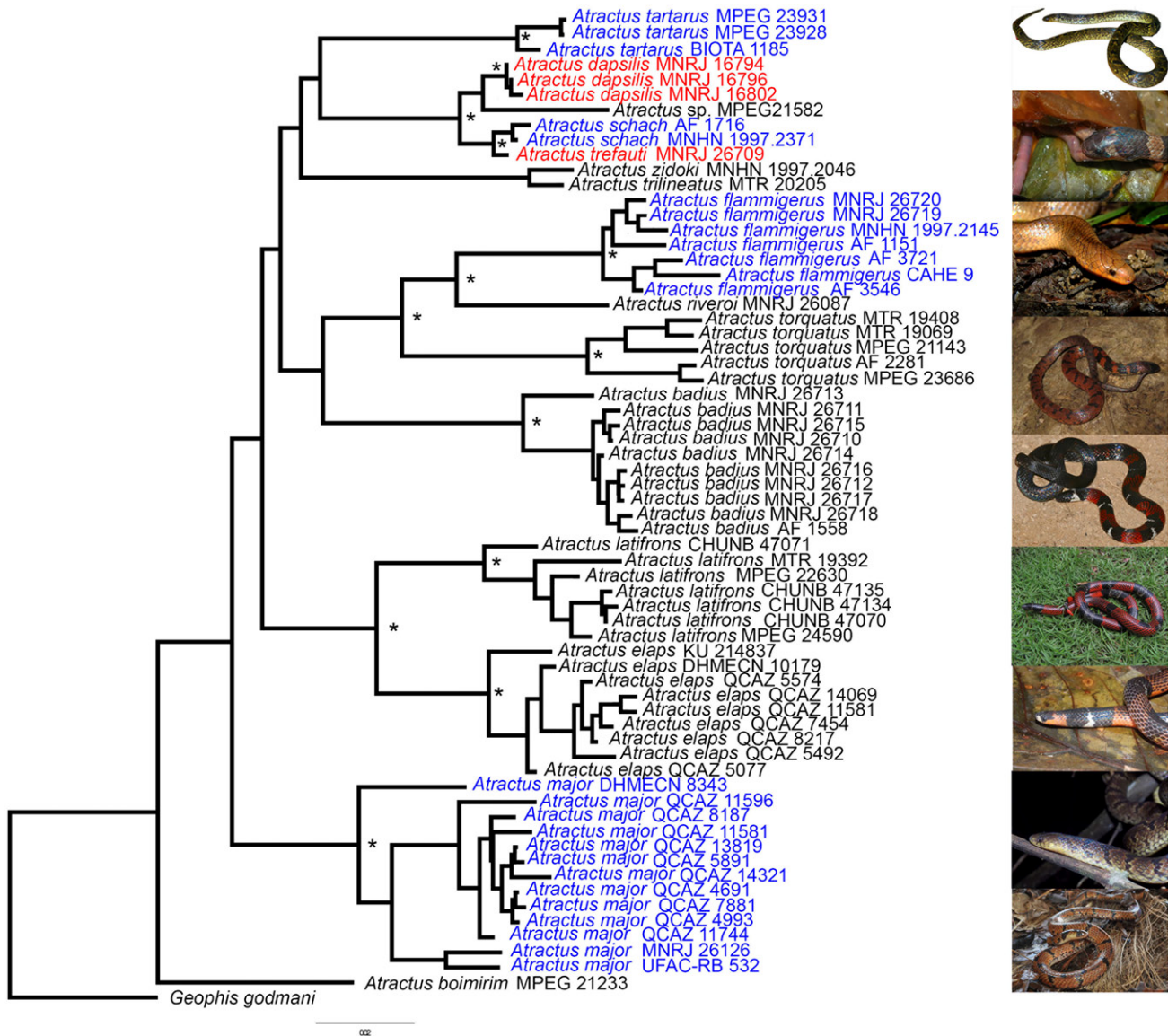


Fig. 1. Phylogeny of *Atractus* from the Guiana Shield. Maximum clade credibility tree obtained from a Bayesian analysis of three mitochondrial and three nuclear genes. Red colour indicates new species described here. Blue colour indicates species formerly assigned to the *Atractus flammigerus* group. Asterisks indicate high posterior probabilities (>0.95). Photographs from top to bottom: *A. tartarus* (R. Bérnils), *A. schach* (C. Marty), *A. flammigerus* (S. Sant), *A. torquatus* (M. Sena), *A. badius* (B. Dupont), *A. latifrons* (P.R. Melo-Sampaio), *A. elaps*, *A. major* (P.R. Melo-Sampaio) and *A. boimirim* (M.S. Hoogmoed).

species of a weakly supported clade (PP= 0.5) containing an unnamed Amazonian species, *Atractus schach* and two new species from the GS (described in taxonomic section).

A distinct clade is formed exclusively by *Atractus badius* (PP = 0.3), confirming its uniqueness and corroborating that the 'coral colour pattern' is not related only to *A. elaps* group. *Atractus torquatus* is recovered as a maximally supported sister species of a clade comprising *A. flammigerus* and *A. riveroi*. External morphology and hemipenis (when available), are in agreement with our concatenated analysis, and the

combined results allow us to clarify the status of *A. schach* and three new species from GS we intend to describe herein.

Taxonomic account

Atractus schach (Boie, 1827)
(Fig. 2)

Brachyorrhos schach F. Bóie, 1827; Isis Von Oken 1827:540. *Calamaria badia* – Schlegel, 1837; Essai sur la Physionomie des Serpens Partie:35. (part.)



Fig. 2. (1) Lectotype RMNH 119a and (2) paralectotype RMNH 119b of *Atractus schach*. Photo by Marinus S. Hoogmoed.

Rhabdosoma badius – Duméril, Bibron & Duméril, 1854; *Erpétologie Générale* Livr. 7:95. (part.) *Atractus badius* – Boulenger, 1894; *Catalogue of the Snakes in the British Museum* 2:309 (part.).

Lectotype. Adult male, RMNH 119a, provenance given as 'Guiana'. Hoogmoed (1980) restricted the type locality to Mamadam (4°56'N, 55°33'W; 33 m above sea level, hereafter asl), Saramaca River, Sipaliwini, Suriname (photos examined).

Paralectotype. Young male, RMNH 119b, same data of lectotype (photos examined).

Diagnosis. *Atractus schach* is distinguished from all congeners by the following combination of characters: (1) smooth dorsal scale rows 17/17/17; (2) postoculars two; (3) loreal moderately long; (4) temporal formula 1 + 2; (5) supralabials seven, third and fourth contacting eye; (6) infralabials eight, first four contacting chinshields; (7) maxillary teeth seven; (8) gular scale rows three; (9) two preventrals; (10) ventrals 148–150 in females, 142–151 in males; (11) subcaudals 19–21 in females, 25–32 in males; (12) in preservative, dorsum olive brown with a series of black regular bands until midbody when becomes alternated dark greyish brown blotches separated by a vertebral line; (13) in preservative, venter cream with two parallel rows of sepia dots or square spots; (14) small body size in female (maximum 260 mm SVL) and in male (maximum 275 mm SVL); (15) moderately long tail both in female

(10–11.3% SVL) and male (10–14% SVL); (16) hemipenis strongly bilobed, slightly semicapitate and semicalyculate.

Comparisons. We restricted the comparisons by geographic proximity due to regionalization and putative endemism of GS snake. Thus, *Atractus schach* differs from *A. aboiporu* sp. nov., *A. elaps*, *A. latifrons*, *A. insipidus*, *A. tamessari*, and *A. trilineatus* by having 17 dorsal scale rows (vs. 15 dorsal scale rows). Regarding the GS species with 17 dorsal scales rows, *Atractus schach* differs from *A. badius* in its dorsal olive-brown colouration with greyish brown transversal bands, and cream to buff ventral colouration with scattered sepia dots (vs. 'coral colour pattern' with black diads separated by cream bands, venter immaculate cream anteriorly, followed by square dark brown dots from midbody to posterior region of belly). *Atractus schach* is distinguished from *A. flammigerus* by SVL < 300 mm in both sexes and absence of keeled dorsal scales near cloaca (vs. adult SVL > 300 mm and presence of keels on dorsal scale rows in *A. flammigerus*); from *A. torquatus* by having SVL < 300 mm in both sexes two postoculars and < 33 subcaudals (vs. one postocular and 34–47 subcaudals in females, 35–53 in males in *A. torquatus* from GS; Passos & Prudente, 2012); from *A. zidoki* by having dorsal scales without apical pits and supra-cloacal tubercles, olive-brown dorsum with dark greyish brown bands and bilobed hemipenis (vs. presence of apical pits and/or supracloacal tubercles on the dorsal scales, light brown dorsum with longitudinal series of paravertebral spots and unilobed hemipenis in *A. zidoki*). For the comparisons between *A. schach* and the new species see section 'comparisons' respectively for each species.

Redescription. Adult male AF 1716. coll. A. Fouquet, E. Courtois and J.-P. Vacher, 26 February 2014, Saül, crique Limonade (3°33'45.3"N, 53°12'37.7"W; 229 m asl), French Guiana. SVL 260 mm, tail length 35 mm (13.4% SVL); head slightly distinct from body; head length 7.8 mm (3% SVL); head width 6.2 mm (79.5% head length); rostral-orbit distance 3.3 mm; nostril-orbit distance 2.5 mm; interorbital distance 3.9 mm; head rounded in lateral view; snout rounded in dorsal view, truncate in lateral view; canthus rostralis poorly defined; rostral subtriangular in frontal view, 1.9 mm wide, 1.1 mm high, visible in dorsal view; internasal 0.9 mm long, 1.0 mm wide; internasal suture sinistral with respect to prefrontal suture; prefrontal 2.5 mm long, 2.1 mm wide; supraocular subtrapezoidal, 1.4 mm long, 1.2 mm wide at broadest point; frontal pyramidal, 2.3 mm long, 3.1 mm wide; parietal 4.1 mm long, 2.8 mm wide; nasal entirely divided, nostril well-divided

in both parts; prenasal 1.0 mm high, 0.5 mm long; post-nasal 1.0 mm high, 0.6 mm long; loreal 2.1 mm long, 0.7 mm high; second and third supralabials contacting loreal; third and fourth supralabials entering the orbit; eye diameter 1.25 mm; pupil rounded; two postoculars; upper postocular 0.6 mm long, 0.7 mm high; lower postocular 0.7 mm long, 0.9 mm high; temporal formula 1+2; first temporal 1.8 mm long, 1.4 mm high; upper posterior temporals 3.3 mm long, 1.0 mm wide; supralabials seven, third and fourth contacting eye; first supralabial shorter in height and length (0.7 & 0.5 mm) than second (1.0 & 0.8 mm); third supralabial pentagonal, taller (1.2 mm) and longer (2.0 mm) than second; sixth supralabial as tall as third; seventh as long as third (2.0 mm) supralabial; symphyseal subtriangular, 1.7 mm wide, 0.4 mm long; first pair of infralabials in contact medially, preventing symphyseal-chinshields contact; infralabials seven, first four contacting chinshields; chinshields each 3.5 mm long, 1.4 mm wide; gular scale rows three; three preventrals; ventrals 142; subcaudals 26; dorsal scale rows 17/17/17, lacking apical pits and supracloacal tubercles; midbody diameter 6.9 mm (2.8% SVL); caudal spine 1.2 mm long, larger than last subcaudal scale (0.9 mm). Retracted hemipenis extends to level of 11th subcaudal, bifurcated at the level of 8th subcaudal. Maxillary bone arched upward anteriorly in lateral view, ventral portion curved anteriorly and nearly flattened in mid to posterior portion; maxillary teeth five, angular in cross section, robust at base, narrower at apices, slightly curved posteriorly, similar in size and spacing; maxillary diastema absent or indistinct from interspaces; lateral process of maxilla well developed.

Dorsum of head dark greyish brown with incomplete collar olive-brown parietals and raw umber suture between parietals extending for eight dorsals long; anterior edges of first four supralabials cream, except for fifth and sixth, in which pigmentation is mostly uniform dark greyish brown; lateral sides of head almost completely dark greyish brown including postocular and anterior temporal; cream infralabials and gular region with sepia spots, except for last two infralabials that are almost completely cream; venter cream to buff with a few dispersed sepia dots on lateral region of ventral scales; ventral surface of tail straw yellow with irregular cream dots; dorsal ground colour olive-brown with 25 conspicuous dark greyish brown bands 1–3 scales long, connected along vertebral axis or not, with sepia narrow vertebral line sometimes inconspicuous covering one scale row width from parietal scale into tip of tail; pale interspaces between dark greyish brown bands often covering five scales long; first dorsal scale row cream, with sepia pigments contacting ventrals; dorsal surface

of tail olive brown with four conspicuous bands; tip of tail olive brown.

Referred material. French Guiana: Orstom 141 from Mana. MNHN 1997.2371 from Camp de Saint-Eugène. MNHN 1997.2481 no specific locality. MNHN 2002.615 from Nouragues. AMNH 139922 no specific locality. RMNH 38072 from Petit Saut, Sinnamary River. Suriname: RMNH 12683 from km 121 road to Brownsberg mountains. SMNS 2664 from Gonini camp.

Hemipenial morphology. Organ *in situ* (entirely retracted) extends to level of 11th subcaudal and bifurcates at level of 9th subcaudal ($n=1$). Fully everted and almost maximally expanded hemipenis renders a strongly bilobed, slightly semicapitate, and semicalyculate organ (Fig. 8.1); lobular region as wide as hemipenial body; lobes centrifugally oriented, attenuated with rounded apices; lobes asymmetrical with right lobe longer than left; lobes uniformly covered with spinulate calyces on both sides of hemipenis; spinules replaced by irregular papillae toward apices of lobes; capitular groove indistinct on the sulcate side of and little evident on the asulcate side of organ; basal and lateral regions of capitulum with irregular rows of spinulate calyces; hemipenial body elliptical covered with enlarged hooked spines; larger spines generally located laterally below sulcus spermaticus bifurcation; distal region of hemipenial body on maximally expanded organ with rows of spines concentrated in the middle of asulcate face; sulcus spermaticus bifurcates approximately on the 30% of organ length with each branch straight-sided, running to tip of lobes; sulcus spermaticus margins relatively thick at level of division and along the capitular region; sulcus spermaticus not bordered by spinules; basal naked pocket restricted to most basal region of hemipenial body; proximal region of hemipenis covered with few dispersed spinules and longitudinal plicae.

Quantitative variation. ($n=10$). Largest female 260 mm SVL, 26 mm TL; largest male 260 mm SVL, 35 mm TL; tail 10–11.3% SVL in females, 10–14% SVL in males; ventrals 148–150 (mean = 149; $n=2$; SD = 1.41) in females, 133–151 (mean = 145; $n=8$; SD = 5.35) in males; subcaudals 19–21 (mean = 20; $n=2$) in females, 25–32 (mean = 28.5; $n=5$) in males; supralabials seven ($n=2$ sides) or eight ($n=4$ sides); infralabials eight ($n=8$ sides) or nine ($n=4$ sides); preventrals three ($n=3$); adult midbody diameter 8.0–8.3 mm; maxillary teeth five ($n=1$), six ($n=2$ sides), or seven ($n=3$ sides).

Distribution. *Atractus schach* occurs in lowlands of Guyana (Cole, Townsend, Reynolds, MacCulloch, & Lathrop, 2013; this study), French Guiana (Chippaux, 1986; Starace, 1998; Vidal et al., 2000; this study) and Suriname (Hoogmoed, 1980; van Lidth de Jeude, 1904).

Remarks. Retracted hemipenis was described by Hoogmoed (1980). All known localities of *A. schach* are in the northern part of Tumucumaque massif.

Atractus dapsilis sp. nov.

(Figs 3, 4)

Atractus badius var. E (Boulenger, 1894 p. 309). *Atractus schach* (Martins & Oliveira, 1993, p. 32, fig. 4d, 6b; Martins & Oliveira, 1998, p. 97, plate 22; Fraga et al., 2013, p. 158; Morato et al., 2014, p. 93; Morato et al., 2018, p. 10). *Atractus snethlageae* (Zimmerman & Rodrigues, 1990; Martins & Oliveira, 1993, p. 34,

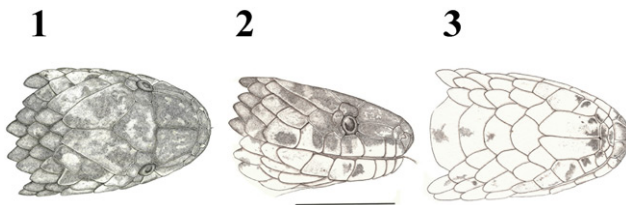


Fig. 3. Dorsal (1), lateral (2) and ventral (3) views of head of the holotype of *Atractus dapsilis* (MNRJ 14914) from Oriximiná, Pará, Brazil.



Fig. 4. Distinct colouration in *Atractus dapsilis* paratypes. (1) MNRJ 14912 and (2) MNRJ 14911.

fig. 4e, 6c; Martins & Oliveira, 1998, p. 97, plate 23; Fraga et al., 2013, p. 160; Morato et al., 2014, p. 94; Morato et al., 2018, p. 10; Schargel et al., 2013, p. 465).

Holotype. Adult male MNRJ 14914: coll. E. G. Pereira and team, 1 February 2007, Platô Teófilo, Flona Saracá-Taquera (1°42'51.6"S, 56°24'34.0"W), alt. 97 m asl, Oriximiná, Pará, Brazil.

Paratypes. All from Brazil. Adult females ($n=15$) PARÁ: Oriximiná MNRJ 14913: coll. E. G. Pereira and team, 30 January 2007. MNRJ 14915: coll. E. G. Pereira and team, 30 January 2007. MNRJ 16799: coll. R. R. Pinto and team, 19 March 2008. MNRJ 16801: coll. R. R. Pinto and team, 20 March 2008. MNRJ 16802: coll. R. R. Pinto and team, 30 June 2008. MNRJ 16803: coll. R. R. Pinto and team, 1 June 2008. MPEG 23759: coll. F. L. Trein, 12 August 2009. MPEG 21570: coll. R. R. Carvalho Jr., 20 May 2006. IBSP 87633: coll. S. Morato, 1 March 2014. MNRJ 16796: coll. R. R. Pinto and team, 8 March 2008. Terra Santa INPA-H 31489: coll. Unknown, 2 August 2011. Amazonas: Manaus MZUSP 3713 coll. K. Lenko, September 1962 (3°07'00.0"S, 60°00'00.0"W) atl. 42 m asl. Rio Preto da Eva MZUSP 8659 coll. B. Zimmerman, 1985, Reserva 41 – INPA/WWF (2°25'00.0"S, 59°43'00.0"W) alt. 81 m asl. Presidente Figueredo MPEG 17426 coll. Rescue Team, 26 January 1988. MPEG 17427 coll. Sônia, 27 January 1988; MPEG 17539 coll. Rescue Team, 11 May 1988.

Adult males ($n=24$) PARÁ: Oriximiná MNRJ 14910: coll. E. G. Pereira and team, 2 February 2007 (1°46'24"S, 56°31'57"W) alt. 130 m asl. MNRJ 14911: coll. E. G. Pereira and team, 5 December 2006. MNRJ 14912: coll. E. G. Pereira and team, 4 December 2006. MNRJ 16794: coll. R. R. Pinto and team, 13 March 2008. MNRJ 16795: coll. R. R. Pinto and team 16 March 2008 (1°27'57"S, 56°22'36"W), alt. 180 m asl. MNRJ 16797: coll. R. R. Pinto and team, 19 March 2008. MNRJ 16798, 16800: coll. R. R. Pinto and team, 19 March 2008. MNRJ 16804: coll. R. R. Pinto and team, 3 July 2008. MPEG 20782: coll. Unknown, 15 November 2003. MPEG 23505: coll. S. Morato, 12 May 2009. MPEG 23760: coll. F. L. Trein, 25 August 2009. MPEG 21569: coll. R. R. Carvalho Jr., 8 May 2006. MPEG 21712–13: coll. E. G. Pereira and team, 31 January 2007. Terra Santa MNRJ 17953–54: coll. F.E. Pimenta and D.M. Morais, 4 to 6 February 2009. Amazonas: Manaus INPA-H 18466 coll. R. de Fraga, 20 November 2006; INPA-H 32271 coll. Unknown, 12 May 2004; INPA-H 32348 coll. Unknown, 11 November 2012, all from Reserva Florestal Adolpho Ducke (2°57'47.7"S, 59°55'22.5"W) alt. 111 m asl. Rio

Preto da Eva MZUSP 9501 *coll.* B. Zimmerman, 9 March 1987, Reserva 41 – INPA/WWF (2°25'00.0"S, 59°43'00.0"W) alt. 81 m asl. IBSP 49430 Reserva Campina – km 60, Manaus-Caracará highway (2°30'00"S, 60°00'00"W) alt. 132 m asl; Presidente Figueredo MPEG 17495 *coll.* Rescue Team, 26 March 1988. MPEG 17568 *coll.* Rescue Team, 28 May 1988, all from Balbina (1°55'10.0"S, 59°28'08.7"W) alt. 29 m asl.

Referred material. IMTM 1061 without data, Manaus. IMTM 1678, 1440, 1378, 1501, 1563, 1354 without data, Presidente Figueredo. RMNH 26020 *coll.* H. Lima and team. 10 October 1991 and RMNH 26021 *coll.* B. Santos and team, 28 October 1991, all from Pitinga river, Presidente Figueredo (1°24'22.1"S, 59°36'43.7"W) alt. 41 m asl.

Diagnosis. *Atractus dapsilis* is distinguished from all congeners by the combination of the following characters: (1) smooth dorsal scale rows 17/17/17; (2) postoculars two; (3) loreal long; (4) temporal formula 1 + 2; (5) supralabials seven, third and fourth contacting eye; (6) infralabials eight, first four contacting chinshields; (7) six or seven maxillary teeth; (8) gular scale rows three; (9) prefrontals three; (10) ventrals 167–182 in females, 152–166 in males; (11) subcaudals 21–26 in females, 30–37 in males; (12) in preservative, dorsum beige to pale brown with a series of dark brown regular bands (21–40 in females, 19–32 in males), some of which are in contact dorsomedially or black with pale bands (morphotype more frequent in males); (13) in preservative, venter pale cream with brown dots forming an inconspicuous midventral line; (14) moderate body size in females (maximum 500 mm SVL) and in males (maximum 360 mm SVL); (15) small tail in females (7.3–10% SVL), moderately long in males (13.3–17.6% SVL); (16) hemipenis strongly bilobed, semicapitate, and semicaliculate.

Comparisons. *A. dapsilis* differs from *A. aboiporu*, *A. elaps*, *A. latifrons*, *A. insipidus*, and *A. trilineatus* by having 17 dorsal scales rows (vs. 15 dorsals). Regarding species with 17 dorsal scales rows, *Atractus dapsilis* differs from *A. badius* in its dorsal colouration being uniformly black with reddish bands or cinnamon with dark bands (Fig. 4), its ventral colouration with scattered brown spots and <38 subcaudals in males (vs. dorsum with black dyads separated by cream bands; belly immaculate anteriorly, followed by square black spots posteriorly; >40 subcaudals in males); differs from *A. favae* by having contact between first pair of infralabials and chinshields and moderate tail <20% SVL (vs. first

pair of infralabials separated from chinshields by first pair of infralabials and tail >22% SVL in *A. favae*); from *A. flammigerus* by lacking keels on the dorsal scales and seven supralabials (vs. keels on the dorsal scales and eight supralabials in *A. flammigerus*); from *A. torquatus* by having two postoculars (vs. one in *A. torquatus* from GS; Passos and Prudente 2012); from *A. zidoki* by having smooth dorsal scales without apical pits, six or seven maxillary teeth and bilobed hemipenis (vs. dorsal scales with apical pits, four or five maxillary teeth and unilobed hemipenis in *A. zidoki*); from *A. snethlageae* by having 167–182 ventrals in females, 152–166 in males; tail 7–10% SVL in females, 13.6–17.4% SVL in males (vs. 147–160 ventrals in females, 137–155 in males; 8.3–11.3% SVL in females, 13.3–16% SVL in males of *A. snethlageae*). *Atractus dapsilis* is closely related (Fig. 1) and morphologically similar to *A. schach* (at least, the pale morph). However, *A. dapsilis* is distinguished from *A. schach* by having 300–451 mm SVL in females and 250–360 mm SVL in males, and more than 152 ventrals in both sexes (vs. maximum SVL 275 mm, < 151 ventrals in both sexes in *A. schach*).

Description of the holotype. Adult male, SVL 307 mm, TL 47 mm (15.3% SVL); head slightly distinct from body; head length 8.3 mm (2.7% SVL); head width 6.4 mm (2.1% head length); rostral–orbit distance 3.5 mm; nostril–orbit distance 2.8 mm; interorbital distance 4.1 mm; head rounded in lateral view; snout rounded in dorsal view, truncate in lateral view; canthus rostralis little conspicuous; rostral subtriangular in frontal view, 2.1 mm wide, 0.9 mm high, well visible in dorsal view; internasal 0.8 mm long, 0.9 mm wide; internasal suture sinistral with respect to prefrontal suture; prefrontal 2.8 mm long, 2.2 mm wide; supraocular ovoid (left) and pentagonal (right), 1.2 mm long, 1.0 mm wide at broadest point; frontal pyramidal, 2.8 mm long, 2.9 mm wide; parietal 4.6 mm long, 2.7 mm wide; nasal entirely divided, nostril well-divided in both parts; prenasal 0.9 mm high, 0.6 mm long; postnasal 1.1 mm high, 0.7 mm long; loreal 2.2 mm long, 0.9 mm high; second and third supralabials contacting loreal; third and fourth supralabials entering the orbit; eye diameter 1.2 mm; pupil rounded; two postoculars distinct in height, lower less tall than upper; upper postocular 0.8 mm long, 1.1 mm high; lower postocular 0.6 mm long, 0.9 mm high; temporal formula 1 + 2; first temporal 2.2 mm long, 1.2 mm high; upper posterior temporals 3.2 mm long, 1.1 mm wide; supralabials seven, third and fourth contacting eye; first supralabial less tall (0.9 mm high) than second (1.1 mm high) and smaller in length (0.6 mm) than second (0.8 mm); third supralabial pentagonal,

taller (1.2 mm) and longer (2.1 mm) than second; sixth supralabial taller (1.5 mm); seventh longer than third (2.5 mm) supralabial; symphyseal subtriangular, 1.9 mm wide, 0.4 mm long; first pair of infralabials prevent symphyseal–chinshields contact; infralabials eight, first four contacting chinshields; chinshields 3.6 mm long, 1.4 mm wide; gular scale rows three (Fig. 3); prementals three; 155 ventrals; subcaudals 32/32; dorsal scale rows 17/17/17, lacking apical pits and supracloacal tubercles; mid-body diameter 8.4 mm (2.7% SVL) caudal spine 1.7 mm long, larger than last subcaudal scale (1.0 mm). Retracted hemipenis extends to the level of 11th subcaudal and bifurcated at 9th. Maxillary bone arched upward anteriorly in lateral view, ventral portion curved anteriorly and nearly flattened in mid to posterior portion; maxillary with seven teeth; teeth angular in cross section, robust at base, narrower at apices, slightly curved posteriorly; teeth similar in size and spacing; last teeth slightly smaller and similarly spaced as anterior ones; maxillary 'diastema' absent or indistinct from interspaces; lateral process of maxilla well developed.

Dorsum of head Vandyke brown with X-shaped olive brown interparietal band; extending equivalent to six dorsal scales long; background of body cinnamon; ventral edges of supralabials cream along border of mouth; lateral sides of head almost completely Vandyke brown to the level of postocular and anterior temporal; posterior lower temporal cream, forming pale occipital area on lateral sides of head; first four infralabials and gular region spotted with Vandyke brown marks, four last infralabials almost completely pale; venter cream with dark brown dots concentrated on midventral region of belly, forming a conspicuous longitudinal stripe; ventral surface of tail cream with drab dots irregularly disposed on subcaudals until level of tip of retracted hemipenis; dorsal ground colour cinnamon with 25 conspicuous sepia bands (0.5–3 scales long), connected to opposite marks until midbody when become alternated; a dark vertebral line sometimes inconspicuous covering one scale row in width from midbody to tip of tail; pale interspaces (four to five scales long) between dark brown bands with irregular dark brown spots concentrated on the paraventral region and, eventually, connected to transverse bands; first dorsal scale row mostly pale cream with dark brown pigmentation concentrated on ventral portion in contact with ventrals; dorsal surface of tail pale brown with conspicuous lateral dark brown spots (sometimes similar to lines); tip of tail dark brown.

Colour pattern variation (Fig. 5). The colour patterns of paratypes agree in general with that described for the holotype with minor variation in the dorsal ground

colour from tawny olive to drab spotted with raw umber to olive brown blotches. Although the dark morph is associated in our sample mostly with males (MNRJ 14910–11, 16794–95, 17953–54. MPEG 21569, 23760), there are at least two females (INPA-H 31489 and MPEG 21570) with such a pattern. The dark morph is as follows: dorsum dark greyish brown to sepia with cinnamon bands (half-scale to three scales long); olive-brown interparietal band; venter cream with raw umber dots increasing in size and number after midbody; ventral surface of tail darker than belly due to higher concentration of raw umber dots on midline with lateral portions of subcaudals predominantly cream.

Quantitative variation (n = 55). Largest female 500 mm SVL, 40 mm TL; largest male 360 mm SVL, 48 mm TL; tail 7–10% SVL in females, 13.6–17.4% SVL in males; ventrals 167–182 (mean 173.3; $n = 23$; $SD = 4.3$) in females, 152–163 (mean 159.5; $n = 32$; $SD = 3.7$) in males; subcaudals 21–26 (mean 23.0; $n = 23$; $SD = 1.7$) in females, 30–37 (mean 33.4; $n = 32$; $SD = 1.9$) in males; supralabials seven ($n = 99$ sides) or eight ($n = 9$ sides); infralabials seven ($n = 11$ sides) or eight ($n = 89$ sides); prementals two ($n = 4$), three ($n = 45$), or four ($n = 6$); adult midbody diameter 7.8–12.0 mm; maxillary teeth six ($n = 15$ sides) or seven ($n = 14$ sides). MNRJ 14911 possesses an azygous scale between internasals and prefrontals.

Variation in hemipenial morphology (n = 6). Organ *in situ* (retracted) extends to the level of 10–12th subcaudal and bifurcate at level of 8th or 9th subcaudal. Fully everted and maximally expanded hemipenis rendered a strongly bilobed, semicapitate, and semicalyculate organ (Fig. 8.3–8); lobular region slightly wider than hemipenial body; lobes nearly attenuate, conical and centrifugally oriented; lobes approximately symmetrical and uniformly covered with spinulate calyces on both sides of hemipenis; calyces on distal region of lobes ornamented with irregular papillae toward apices of lobes; interlobular region nude at base; lobular portion on both faces of organ and basal region of capitulum, except for the intrasulcar region, conspicuously ornamented with transverse spinulate flouces; intrasulcar region of sulcate side of hemipenis with predominantly irregular calyces; regular flouces distributed along both sides of organ but more conspicuous laterally; flouces formed by loss of vertical walls of calyces on laterodistal regions of both faces of capitulum; capitular groove well evident on both sides of hemipenis; capitulum covering ~40% of hemipenial length; hemipenial body elliptical and surrounded with large hooked spines; larger spines



Fig. 5. Colour in life of *Atractus dapsilis*. Photos: L. Mendes (1–4) and M. Martins (5–8).

generally located laterally below sulcus spermaticus bifurcation; distal region of hemipenial body on maximally expanded organs with rows of spines concentrating in the middle of asulcate face; sulcus bifurcates in the middle-length of organ with each branch centrifugally oriented, running to tip of lobes;

sulcus spermaticus margins relatively thick at level of division and capitular region; sulcus spermaticus not bordered by spinules; basal naked pocket long, almost reaching level of bifurcation of sulcus spermaticus; proximal region of hemipenis with few dispersed spinules and longitudinal plicae (Fig. 8C–F).

Etymology. The specific epithet '*dapsilis*' is a neuter Latin adjective meaning abundant or bountiful. We use this name in reference for the relative local abundance of the new species, which unlike many other congeners is herein described based on a large sample size.

Distribution. *Atractus dapsilis* occurs in terra firme Amazonian rain forest, ranging from plateaus (29–180 m asl) in the Brazilian States of Amazonas (municipalities of Manaus, Presidente Figueredo, and Rio Preto da Eva) and Pará (municipalities of Oriximiná and Terra Santa). The natural history of this species is well reported by Martins and Oliveira (1993).

Atractus trefauti sp. nov.
(Figs 5, 6.5–6)

Atractus flammigerus snethlageae (Cunha & Nascimento, 1983; in part)

Holotype. Adult male, MNRJ 26709 (field number AF 814): coll. A. Fouquet, E. Courtois and M. Dewynter, 18 December 2012, Route de l'Est N2, Roura, French Guiana, (4°29'19.7"N, 52°21'01.4"W; 43 m asl).

Paratypes. Females ($n=3$) MPEG 25788: coll. U. Gallatti, D. Silvano and B. Pimenta, 9 November 2000, Serra do Navio, Amapá, Brazil. MPEG 16382: [formerly paratype of *Atractus flammigerus snethlageae*] coll. J. Luiz, 17 July 1977, Serra do Navio, Amapá, Brazil. MNHN 2015.56: coll. F. Starace, 16 April 2015, Réserve de la Trinité, Mont Tabulaire, French Guiana. Males ($n=2$) MPEG 21354–55: coll. T.A. Gardner and M.A. Ribeiro-Júnior, 21 March 2005, Monte Dourado (1°1'32"S, 52°54'17"W), Almeirim, Pará, Brazil.

Referred specimens ($n=2$). Adult male, AMNH-R 139916 and juvenile male, AMNH-R 139923: coll. Unknown, between 15 July to 19 September 1993, no specific site, French Guiana.

Diagnosis. *Atractus trefauti* can be distinguished from all congeners by the unique combination of the

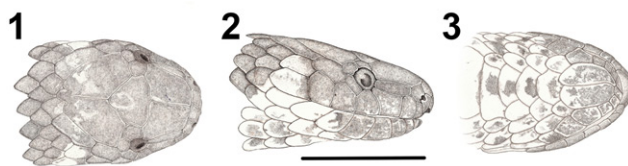


Fig. 6. Dorsal (1), lateral (2) and ventral (3) views of the holotype of *Atractus trefauti* (MNRJ 26709) from Roura, French Guiana.

following characters: (1) smooth dorsal scale rows 17/17/17; (2) postoculars two; (3) loreal moderately long; (4) temporal formula 1 + 2; (5) supralabials seven, third and fourth contacting eye; (6) infralabials eight, first four contacting chinshields; (7) maxillary teeth five to seven; (8) gular scale rows three; (9) three prefrontals; (10) ventrals 153–158 in females, 139–149 in males; (11) subcaudals 21–24 in females, 24–29 in males; (12) in preservative, dorsum black with a series of white regular bands one scale long, interrupted on vertebral scales, 15–26 in females, 27–40 in males; (13) in preservative, venter pale cream with scattered brown dots almost forming a midventral line, increasing in size in the posterior half of body; (14) small body size in both sexes (maximum SVL 332 mm in females, 295 mm SVL in males); (15) moderately short tail in females (8.3–9.9% SVL), moderately long tail in males (12.2–13.2% SVL); (16) hemipenis slightly bilobed, semicapitate and semicalyculate.

Comparisons. *Atractus trefauti* differs from *A. aboi-poru*, *A. elaps*, *A. latifrons*, *A. insipidus*, *A. tamessari*, and *A. trilineatus* by having 17 (vs. 15) dorsal scale rows. Regarding the species with 17 dorsal scale rows, *A. trefauti* differs from *A. badius* by its dorsal colouration of black with pale brown transverse bands, ventral colouration with scattered brown dots and <30 subcaudals (vs. 'coral colour pattern' with black dyads separated by cream bands; venter immaculate cream anteriorly and with squared black spots from midbody to posterior region of belly; >30 subcaudals); from *A. flammigerus* by having maximum SVL 300 mm in both sexes and absence of keeled dorsal scales near cloaca (vs. SVL > 300 mm in adults, keeled dorsal scales in *A. flammigerus*); from *A. schach* by having a black dorsum with beige bands, black iris (Fig. 7) and well-defined hemipenial capitular groove (vs. olive brown with dark greyish brown bands; light brown iris and indistinct hemipenial capitular groove in *A. schach*) (Fig. 8.1); from *A. torquatus* by having maximum SVL 300 mm in both sexes and two postoculars (vs. SVL <300 mm in adults from both sexes; one postocular in *A. torquatus* from GS; Passos and Prudente, 2012); from *A. zidoki* by having smooth dorsal scales without apical pits, black dorsum with pale brown bands and bilobed hemipenis (vs. apical pits present in dorsal scales, pale brown dorsum with longitudinal series of paravertebral spots and unilobed hemipenis in *A. zidoki*); from *A. snethlageae* by having invariably black dorsal ground colour across age and sex (Fig. 9; our sample comprises both adult and females with no indication of ontogenetic change), 15–18 dorsal beige bands in females and 21–40 in males (vs. dark brown dorsum with 24–34



Fig. 7. Colour in life of *Atractus schach* (1–4) and *Atractus trefauti* (5–6). Photos: F. Starace (1–2), B. Dupont (3), J. P. Vacher (4) and F. Deschandel (5–6).

dorsal pale bands in females and 28–31 in males). *Atractus trefauti* also differs from *A. snethlageae* in having 24–28 subcaudals in males (vs. 29–34 subcaudals *A. snethlageae*).

Description of the holotype (Fig. 6). Adult male, SVL 235 mm, TL 31 mm (13.2% SVL); head slightly distinct from body; head length 7.3 mm (3.1% SVL); head width 5.9 mm (80.2% head length); rostral–eye distance 3.4 mm; nostril–orbit distance 2.4 mm; interorbital distance 3.6 mm; head rounded in lateral view; snout rounded in dorsal view, truncate in lateral view; canthus rostralis little conspicuous; rostral subtriangular in frontal view, 1.8 mm wide, 0.7 mm high, well visible in dorsal view; internasal 0.7 mm long, 0.9 mm wide; internasal suture sinistral with respect to prefrontal suture; prefrontal 2.2 mm long, 1.9 mm wide; supraocular

subtrapezoidal, 1.1 mm long, 0.8 mm wide at broadest point; frontal pyramidal, 2.4 mm long, 2.7 mm wide; parietal 3.7 mm long, 2.4 mm wide; nasal entirely divided, nostril almost restricted to prenasal; prenasal 0.7 mm high, 0.5 mm long; postnasal 0.9 mm high, 0.7 mm long; loreal 1.8 mm long, 0.7 mm high; second, third, and fourth supralabials contacting loreal on left side; second and third supralabials contacting loreal on right side; eye diameter 1.1 mm; pupil rounded; two postoculars similar in height, lower being longer than upper; upper postocular 0.6 mm long, 0.8 mm high; lower postocular 0.5 mm long, 0.9 mm high; temporal formula 1 + 2; first temporal 1.6 mm long, 1.0 mm high; upper posterior temporals fused, 2.6 mm long, 1.0 mm wide; supralabials seven, third and fourth contacting eye in right side, supralabials eight, fourth and fifth contacting eye in left side; first supralabial shorter (0.7 mm

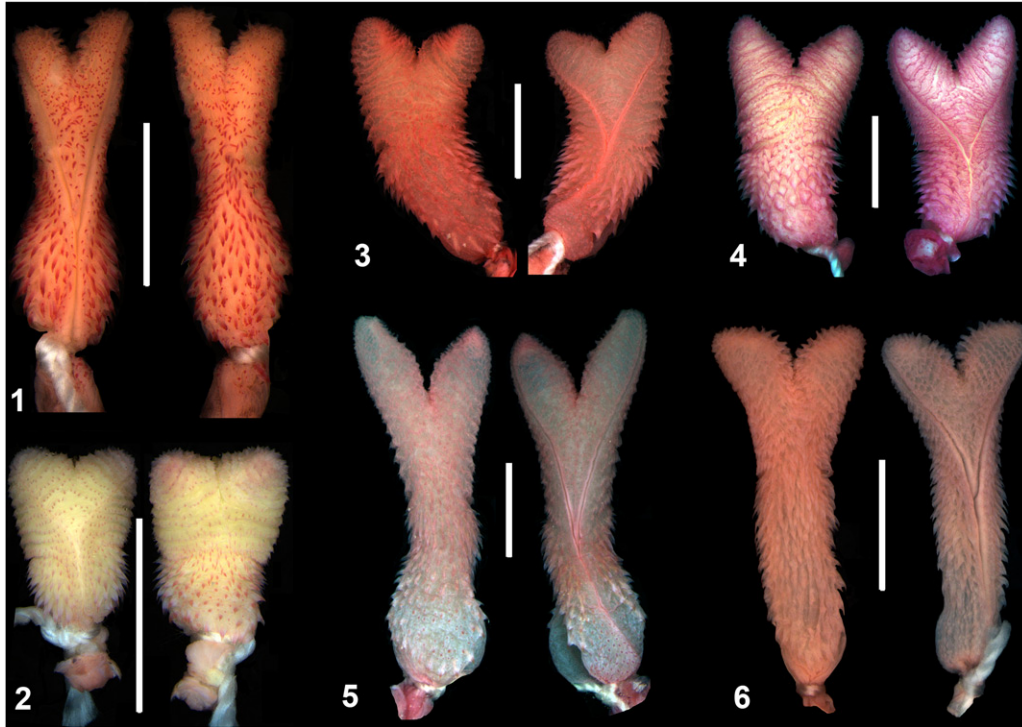


Fig. 8. Hemipenial variation of *Atractus* from GS. Left: asulcated view; Right: sulcated view. (1) *Atractus schach*: (AF 1716) from Saul Limonade, French Guiana. (2) *Atractus trefauti*: Holotype (MNRJ 26709) from Roura, French Guiana. (3–6) *Atractus dapsilis*: (3) Paratype (MNRJ 14911), (4) Paratype (MNRJ 16804), (5) Paratype (MNRJ 14912), (6) Holotype (MNRJ 14914).

high) than second (1.0 mm high) and similar in length; third supralabial rectangular, similar in height and longer (0.6 mm) than second; seventh supralabial taller (1.2 mm) and eighth longer (2.2 mm) than remaining supralabials; symphyisial subtriangular, 1.3 mm wide, 0.4 mm long; first left infralabial preventing symphyisial–chinshields contact; symphyisial contacting right chinshield; infralabials eight, first four contacting chinshields; chinshields 3.0 mm long, 1.1 mm wide; gular scale rows three; preventrals three; ventrals 144; subcaudals 25/25; dorsal scale rows 17/17/17, lacking apical pits and supraclacal tubercles; midbody diameter 6.7 mm (2.8% SVL); caudal spine 1.1 mm long, larger than last subcaudal scale (0.7 mm). Maxillary bone arched upward anteriorly in lateral view, ventral portion curved anteriorly and nearly flattened in mid to posterior portion; maxillary with five teeth; teeth angular in cross section, robust at base, narrower at apices, curved posteriorly; first three teeth larger and more closely spaced; fourth teeth slightly smaller, moderately spaced, similar in size to three anterior ones; last teeth smallest with same spacing to fourth; maxillary 'diastema' absent or indistinct from interspaces between fourth and fifth teeth; lateral process of maxilla well developed.

Dorsum of head black, with dark brown spots (each approximately half a dorsal scale long) covering part of

parietals and upper secondary temporals; dorsal ground colour of lower secondary parietal and last supralabial pale brown, with pale area diagonally disposed; background of head black; edges of first four supralabials pale brown, except for fifth and sixth uniformly black; lateral sides of head completely black to the level of postocular and anterior temporal; posterior lower temporal and last supralabial scales pale brown, forming pale area on lateral sides of head (incomplete nuchal band); infralabials and gular region cream with black dots; belly cream with few dispersed brown dots mostly concentrated on lateral parts of ventrals; ventral surface of tail black with cream dots irregularly disposed along subcaudals; dorsal ground colour black with 27 conspicuous beige bands, one-half to one scale long, the first five separate only by vertebral scale, then alternated; beige bands starting on the second or third dorsal scale row; interspaces between bands four to seven scales long; first dorsal scale row beige with cream pigmentation irregularly disposed on each scale; dorsal surface of tail black with four conspicuous bands; tip of tail black.

Hemipenial morphology. Organ *in situ* (retracted) extends to the level of fifth subcaudal and bifurcates at fourth subcaudal ($n=2$). Fully everted and almost maximally expanded hemipenis rendered a moderately

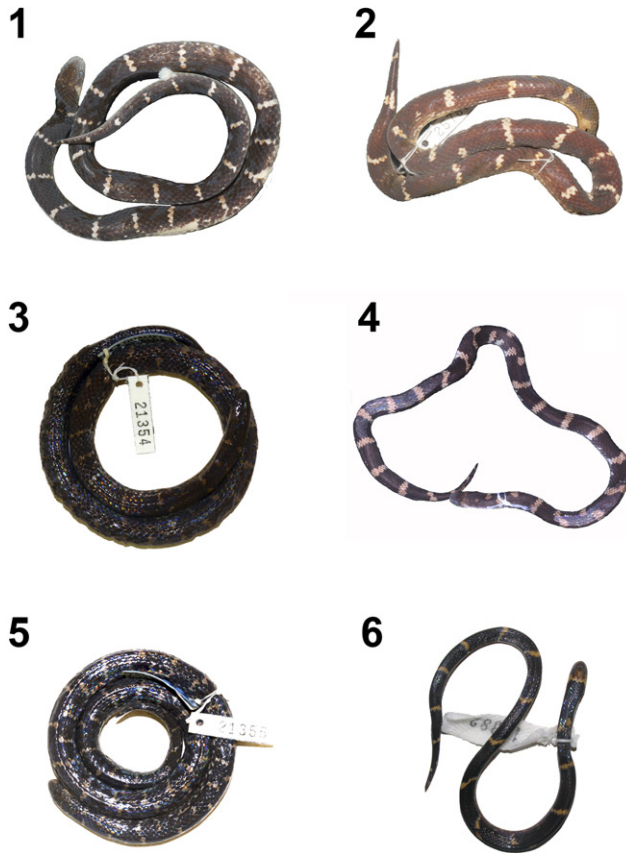


Fig. 9. Morphological variation in *Atractus trefauti*. Left row males: (1) holotype (MNRJ 26709); (3) paratype (MPEG 21354) and (5) paratype (MPEG 21355). Right row females: paratypes: (2) MPEG 25788; (4) MNHN 2015.56 and (6) MPEG 16382.

bilobed, semicapitate and semicalyculate organ (Fig. 8.2); lobular region wider than hemipenial body; lobes symmetrical, rounded and centrifugally oriented; lobes uniformly covered with spinulate calyces on both sides of hemipenis; calyces on distal region of capitulum ornamented with transverse rows of papillae toward apices of each lobe; basal and lateral regions of capitulum with transverse fringes; capitular groove well-defined on asulcate side and less evident on sulcate side of hemipenis; capitulum covering approximately half-length of hemipenial body; hemipenial body elliptical, surrounded with hooked spines; larger spines generally located laterally below sulcus spermaticus bifurcation on sulcate face of organ; distal region of hemipenial body on maximally expanded organs with rows of spines similar size bordering capitulation; sulcus bifurcates for about half-length of organ and each branch centrifugally oriented, running to tip of lobes; sulcus spermaticus deep with margins bordered by relatively thick layer of papillae; sulcus spermaticus bordered by spinules from base of organ to apices of lobes; basal naked pocket extending for almost entire hemipenial body.

Quantitative variation ($n = 5$). Largest female 300 mm SVL, 25 mm TL; largest male 295 mm SVL, 39 mm TL; tail 8.3–9.7% SVL in females; 12.9–13.2% SVL in males, ventrals 153–158 (mean = 156.0; $n = 3$; SD = 2.6) in females, 139–149 (mean = 143.2; $n = 5$; SD = 3.8) in males; subcaudals 21–24 (mean = 22.7; $n = 3$; SD = 1.5) in females, 24–29 (mean = 26.6; $n = 5$; SD = 2.1) in males; supralabials seven ($n = 5$ sides) or eight ($n = 2$ sides); infralabials eight ($n = 5$ sides); pre-ventrals three ($n = 4$) or four ($n = 1$); adult midbody diameter 8.0–8.3 mm; maxillary teeth five ($n = 1$), six ($n = 2$ sides), or seven ($n = 3$ sides).

Etymology. The specific epithet honours Dr Miguel Trefaut Urbano Rodrigues from Universidade de São Paulo (USP) for his extensive contributions in the study of New World herpetofauna, especially with respect to *Atractus* from Guiana Shield.

Distribution and natural history. *Atractus trefauti* is known to occur in lowland sites ranging from Roura, French Guiana, and Amapá and Pará States in Brazil.

Atractus aboiporu sp. nov.

(Figs 10, 11)

Holotype. Adult female, MPEG 25796: coll. U. Galatti, D. Silvano, and B. Pimenta, 9 November 2000, Serra do Navio, Amapá, Brazil.

Paratype. MPEG 25797: same data as holotype. MPEG 19783: coll. U. Galatti and J. A. R. Bernardi, 29 August 2000, Pedra Branca do Amapari, Amapá. (0°51'34"N, 51°52'34"W; 161 m asl).

Diagnosis. *Atractus aboiporu* can be distinguished from all congeners by the unique combination of the following characters: (1) smooth dorsal scale rows 15/15/15; (2) postoculars two; (3) loreal moderately long; (4) temporal formula 1 + 2; (5) supralabials seven, third and fourth contacting eye; (6) infralabials seven, first four contacting chinshields; (7) maxillary teeth seven; (8) gular scale rows three; (9) pre-ventrals two; (10) ventrals 133–135 in females, unknown in males; (11) subcaudals



Fig. 10. Dorsal (1), lateral (2) and ventral (3) views of head of the holotype of *Atractus aboiporu* (MPEG 25796) from Serra do Navio, Amapá, Brazil.

15–16 in females, unknown in males; (12) in preservative, dorsum cinnamon to verona brown with a series of sepia blotches mostly like rhomboidal parallelograms along the vertebral axis; (13) in preservative, venter beige with two rows of sepia dots or square spots, mostly concentrated on the midbody scales; (14) small body size in female (maximum 275 mm SVL); (15) small tail in female (7.6–10.8% SVL).

Comparisons. Among congeners from the Guiana Shield (including highland species), *A. aboiporu* differs from *A. badius*, *A. duidensis*, *A. flammigerus*, *A. latifrons*, *A. riveroi*, *A. steymarki*, *A. trefauti*, *A. schach*, and *A. torquatus* by having 15 dorsal scales rows (vs. 17 scales rows). Considering species with 15 dorsal scales rows, *A. aboiporu* differs from *A. insipidus* and *A. tamessari* by having 135 ventrals, 15 subcaudals (vs. >150 and 24, respectively in both species); from *A. trilineatus* by having a dorsal brown colour brown with conspicuous black vertebral blotches, belly cream with two longitudinal brown stripes, seven supralabials, and seven infralabials (vs. dorsum reddish brown with three conspicuous longitudinal black stripes, belly uniformly cream, eight supralabials, and eight infralabials in *A. trilineatus*). *Atractus aboiporu* shares 15/15/15 dorsal scale rows, dorsal ground colour cinnamon to verona brown with sepia blotches drap-bordered, seven supralabials and seven infralabials only with species distributed south of Amazon River, *A. boimirim* and *A. tartarus*. However, *A. aboiporu* differ from both species by having two parallel rows of sepia spots along the belly (vs. venter uniformly creamish white or scattered with brown dots concentrated on lateral portions of ventral scales, but never forming conspicuous stripes in *A. boimirim* and *A. tartarus*).

Description of the holotype. Adult female, SVL 275 mm, tail length 23 mm (7.6% SVL); head slightly distinct from body; head length 9.4 mm (3.4% SVL); head width 7.2 mm (76.5% head length); rostral–eye distance 3.6 mm; nostril–orbit distance 2.7 mm; interorbital distance 3.8 mm; head rounded in lateral view; snout rounded in dorsal view, truncate in lateral view; canthus rostralis little conspicuous; rostral subtriangular in frontal view, 1.5 mm wide, 1.0 mm high, well visible in dorsal view; internasal 0.8 mm long, 0.9 mm wide; internasal suture sinistral with respect to prefrontal suture; prefrontal 2.5 mm long, 2.1 mm wide; supraocular subtrapezoidal, 1.8 mm long, 1.3 mm wide at broadest point; frontal pyramidal, 3.1 mm long, 2.7 mm wide; parietal 4.3 mm long, 2.7 mm wide; nasal entirely divided, nostril almost restricted to prenasal; prenasal 0.9 mm high, 0.4 mm long; postnasal 0.9 mm high, 0.6 mm long; loreal 2.2 mm long, 0.8 mm high; second and third supralabials

contacting loreal; third and fourth supralabials entering the orbit; eye diameter 1.4 mm; pupil rounded; two postoculars distinct in height, lower being taller than upper; upper postocular 0.7 mm long, 0.6 mm high; lower postocular 0.5 long, 0.9 mm high; temporal formula 1 + 2; first temporal 1.9 mm long, 1.4 mm high; upper posterior temporals 0.9 mm long, 0.6 mm wide; supralabials seven, third and fourth contacting eye; first supralabial less tall (0.7 mm high) than second (1.0 mm high) and smaller in length (0.7 mm) than second (1.0 mm); third supralabial pentagonal, longer (1.4 mm) and taller (2.0 mm) than second; sixth supralabial as tall as third; seventh longer (2.3 mm) than remaining supralabials; symphyseal subtriangular, 1.3 mm wide, 0.4 mm long; first pair of infralabial preventing symphyseal–chinshields contact; infralabials seven, first four contacting chinshields; chinshields 3.8 mm long, 1.4 mm wide; gular scale rows three; three preventrals; ventrals 135; subcaudals 15/15; dorsal scale rows 15/15/15, lacking apical pits and supraocloacal tubercles; midbody diameter 6.7 mm (2.8% SVL); caudal spine 1.1 mm long, larger than last subcaudal scale (0.7 mm). Maxillary bone arched upward anteriorly in lateral view, ventral portion curved anteriorly and nearly flattened in mid to posterior portion; maxillary with seven teeth; teeth angular in cross section, robust at base, narrower at apices, slightly curved posteriorly; teeth similar in size and spacing; last teeth slightly smaller and with same spacing as anterior ones; maxillary 'diastema' absent or indistinct from interspaces between fifth and sixth teeth; lateral process of maxilla well developed.

Dorsum of head cinnamon brown, warm sepia spots contacting eye and covering mesial suture between parietals; dorsal ground colour of lower secondary parietal and last supralabial beige, diagonally disposed; edges of first four supralabials beige anteriorly; lateral sides of head completely cinnamon brown into postocular and anterior temporal; posterior lower temporal and last supralabial scales beige diagonally disposed (triangle-shaped) (Fig. 10). Ventral ground colour of infralabials and gular region mostly cream with brown spots and blotches; brown spots concentrated on labial margins and posterior region of infralabials; chinshields with few dispersed dots; preventral with midventral squared spots; venter beige with two rows of sepia squared spots arranged nearly longitudinally, forming two irregular midventral stripes along body; ventral surface of tail with two lateral rows of sepia with beige irregular midline along subcaudal sutures; dorsal ground colour verona brown with 35 conspicuous sepia blotches with drap borders (half-scale to one scale long), connected along vertebral region; dorsal blotches (five scales wide and three scales long) similar to parallelograms covering



Fig. 11. Morphological variation in *Atractus aboiporu* in dorsal and ventral view. Upper: holotype (MPEG 25796); Middle: paratype (MPEG 25797); Lower: paratype (MPEG 19783).

the five scale rows; interspaces among parallelograms often two scales long; first dorsal scale row cream like ventrals; dorsal surface of tail brown with four conspicuous sepia bands connected along vertebral axis; tip of tail cream (Fig. 11).

Hemipenis. Unknown.

Quantitative variation ($n = 3$). Largest female 275 mm SVL, 23 mm TLL; tail 5.1–7.6% SVL in females; 133–135 (mean 133.7; $n = 3$; SD = 1.2) in females; subcaudals 15–16 (mean 15.3; $n = 3$; SD = 0.6) in females; supralabials seven ($n = 6$ sides); infralabials seven ($n = 6$ sides); prefrontals three ($n = 3$); adult midbody diameter 8.0–8.3 mm; maxillary teeth five ($n = 1$).

Etymology. The specific epithet ‘*aboiporu*’ is a Tupi indigenous name herein used in apposition alluding to the peculiar feeding habits of the new species (*abôî* = earthworm; *poru* = eater), as well as other congeners.

Distribution. Known only from the type locality and Pedra Branca do Amapari, state of Amapá, Brazil.

Discussion

Atractus trefauti, *A. dapsilis*, and *A. schach* are recovered here as members of a robustly supported

monophyletic group consisting exclusively of banded-species endemic to the eastern GS (Fig. 12). Previous molecular datasets using sequences from multiple specimens for single terminals were possibly misleading. For example, Pyron *et al.* (2013) used sequences from two specimens, to create a single terminal for ‘*Atractus schach*’: one from GS and other from Southern Amazon River in the state of Pará. Thus, although a composite terminal or chimaera may improve the support values of some clades recovered in analyses, in this case they are hiding a cryptic biodiversity and phylogenetic relationships. We strongly recommend future molecular phylogenetic studies on *Atractus* use of same specimen for all loci. If data need to be used from multiple specimens of same taxon then it is best if this is not done in a chimaeric way. The pattern of distribution of *A. trefauti* in east GS is like that of *A. flammigerus* (Passos *et al.*, 2017). Some supposedly widespread species of *Atractus* might represent complexes of narrowly distributed and restricted endemic taxa. For example, the disjunct distribution previously thought for *A. zidoki* along both banks of the Amazon River (Cunha & Nascimento, 1984), was subsequently proved to include a distinct species (*A. hoogmoedi* Prudente & Passos, 2010) occurring exclusively south of Amazon River while *A. zidoki* remains restricted to GS (Prudente & Passos, 2010). Moreover, *A. flammigerus*, *A. riveroi*, and *A. torquatus* form a distinct clade with parapatric distributions, with the first restricted to the extreme east portion of GS (Passos *et al.*, 2017). Although *A. torquatus* is the only species occurring south of Amazon River, where it is widely distributed across Amazonia (see Passos & Prudente, 2012; Passos, Kok, *et al.*, 2013), *A. riveroi* is restricted to highlands Tepuis north of the Amazon (Fraga *et al.*, 2017). Although molecular data are unavailable, *Atractus aboiporu*, is described based on a distinctive set of characters that easily distinguish it from other species occurring in the GS, as well as from recently described Amazonian species (*A. boimirim* and *A. tartarus*).

Some pale individuals of *A. dapsilis* resemble *A. schach* but differ from this species by their larger body-size, genital features and higher number of ventral and subcaudal scales. The evolutionary interpretation of the occurrence of sexual dichromatism in the genus *Atractus* remains unclear (see Passos, Lynch, & Fernandes, 2008). Nonetheless, the colour pattern inversion reported herein in *A. dapsilis* is also known in *A. erythromelas* (Passos, Kok, *et al.*, 2013), *A. riveroi* (Fraga *et al.*, 2017; Roze, 1961) and *A. sanctaemartae* (Passos *et al.*, 2008). Recently, de Fraga *et al.* (2017) discussed how poor sampling of species of *Atractus* might lead researchers to hypothesize instances of endemism that are artefactual. Some *Atractus* species are probably more difficult to detect in the field,

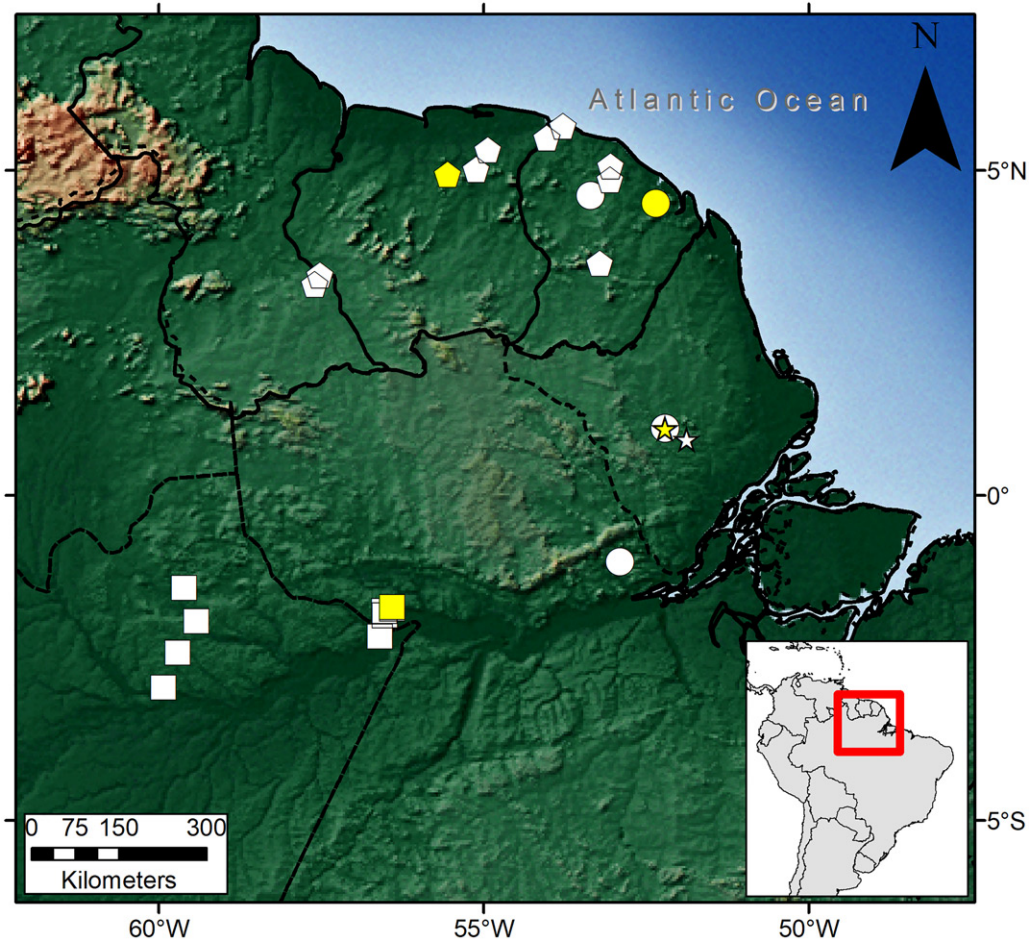


Fig. 12. Known distribution of *Atractus aboiporu* (stars), *A. dapsilis* (squares), *A. schach* (pentagons) and *A. trefauti* (circles). Yellow symbols are type localities. Literature records for *Atractus schach* are based in Hoogmoed (1980), Hoogmoed and Ávila-Pires (1991), Chippaux (1986), Starace (1998), and Vidal et al. (2000).

especially in highlands, where soils, vegetation, and habitus must be adapted to the environmental restrictions (Passos, Kok, et al., 2013) with fewer prey items available, because *Atractus* are earthworm-feeding specialists, this probably limits the population size and consequently its abundance (with direct effects in detectability).

We identified the composite nature of the type series of *A. snethlageae* and have described three distinct species based on the hemipenial morphology, pholidosis, and colouration. We also corroborate GS endemism for *A. schach*. Populations south of the Amazon River previously attributed to *A. schach* (Cunha & Nascimento, 1993; Nascimento et al., 1988) are instead part of a species complex closely related to *A. snethlageae* (PRMS, unpubl. data). However, we refrain from formal taxonomic decisions here, awaiting the results of analyses sampling extensively along the Amazonian lowlands, as well the Andean foothills.

Recent advances in *Atractus* systematics have been contrasting. On one hand, new species have been described

morphologically in detail using large series and through comparisons (e.g., *A. boimirim* and *A. tartarus*; Passos et al., 2016). On the other hand, some species have been described based mostly on molecular phylogenetic analyses, and using small samples, less morphological detail, and limited taxonomic comparisons (*A. cerberus*, *A. esepe*, and *A. pyroni*; Arteaga et al., 2017). In the current ‘biodiversity crisis’ (Wilson, 1985), we need to make species discovery and descriptions faster to improve conservation strategies and provide support to protect areas (Fouquet et al., 2018; Passos et al., 2018). However, we also recommend that even for geographically limited samples positioned on some partial phylogenetic hypotheses, the inference of species boundaries should be based on as much evidence as available, following the congruence between distinct systems of characters and integrating them whenever possible (Padial et al., 2009). Taxonomic instability will not help conservation.

Passos et al. (2016) proposed the *Atractus flammigerus* species group to accommodate *A. tartarus* and

many other banded cis-Andean species, that share a combination of phenotypic characters (mainly from the hemipenial morphology). The tentative inclusions of trans-Andean species should be tested in a most inclusive approach, but probably they will be geographically structured and nested among distinct clades (see Passos *et al.*, 2009; Arteaga *et al.*, 2017). Our study is the most-densely taxon and character sampled systematic investigation of the *Atractus flammigerus* species group thus far, including five out of eight species, and mitochondrial and nuclear markers, as well as morphological data (meristic, morphometric, colour pattern, and genital features). Our results suggest the non-monophyly of this group as originally conceived.

The congruence between distinct systems of characters may solve the limitation of data through integration of primary sources of information using those that have not been exhaustively implemented for the entire genus *Atractus*. For example, the keeled scales above cloaca mentioned for *Atractus flammigerus* in Hoogmoed (1980) arises as a putative robust character that could be useful for taxonomic purposes among the species group. Recently, Passos *et al.* (2017) has employed new techniques such as scale micro-ornamentation and computerized tomography scanning and proved to be successful in distinguishing between species being useful and non-invasive, allowing integrity of type specimens. Among other useful character systems in the *Atractus* taxonomy are the osteology, glands, soft anatomy, scales' macro and micro-ornamentation, and genital features (Passos *et al.*, 2016, 2017), but all these phenotypic systems useful to accommodate species restricting comparisons into small operational groups are virtually unexplored. Currently hypotheses of relationships for the genus *Atractus* are incomplete due to the absence of the majority of Andean species and related genera such as *Geophis* Wagler 1830 and *Adelphicos* (Passos *et al.*, 2013; Passos *et al.*, 2018).

Acknowledgements

We thank M. Wilkinson, D. Gower, E. Shubert, and an anonymous reviewer, who improved the manuscript with valuable suggestions. We also thank A. Kupfer (SMNHS), E. Dondorp (RMNH), L. Vonnahme, and D. A. Kizirian (AMNH), S. Schweiger, G. Gassner, and A. Schumacher (NHW) who provided useful data. F. Starace, B. Dupont, L. Mendes, M. S. Hoogmoed, M. Sena, R. S. Bérnils, S. Sant, J.-P. Vacher, E. Courtois, M. Dewynter, and F. Deschandol helped with images of living specimens. We also thank staff from Reserve Naturelle de la Trinité and Parc Amazonien de Guyane by Access and Benefit Sharing Agreement

(APA no. 973-23-1). We acknowledge support from an 'Investissement d'Avenir' grant managed by Agence Nationale de la Recherche (CEBA, ref.ANR-10-LABX-25-01). We also thank J. C. Silva, local people and staff from Reserva Extrativista Arapixi. SISBIO granted the permit (#51748-1). We thank the Nature Conservation Division and the STINASU for collecting permits in Suriname and colleagues Paul Ouboter and Rawien Jairam.


Funding

PRMS was CAPES fellow (88882.183267/2018-01). PP was supported by Conselho Nacional de Desenvolvimento Científico e Tecnológico (process 302611/2018-5, and 306227/2015-0) and Fundação Carlos Chagas Filho de Amparo à Pesquisa do Estado do Rio de Janeiro (E-26/202.737/2018). Molecular work and fieldwork by OTC was funded by SENESCYT under the 'Arca de Noé' Initiative (PIs: S.R. Ron and OTC).

Supplemental data


Supplemental data for this article can be accessed here: <http://dx.doi.org/10.1080/14772000.2019.1614694>.

ORCID

Paulo Roberto Melo-Sampaio  <http://orcid.org/0000-0003-1858-1643>

Paulo Passos  <http://orcid.org/0000-0002-1775-0970>

Antoine Fouquet  <http://orcid.org/0000-0003-4060-0281>

Ana Lucia Da Costa Prudente  <http://orcid.org/0000-0002-4164-6815>

Omar Torres-Carvajal  <http://orcid.org/0000-0003-0041-9250>

References

- Almeida, P. C., Feitosa, D. T., Passos, P., & Prudente, A. L. C. (2014). Morphological variation and taxonomy of *Atractus latifrons* (Günther, 1868) (Serpentes: Dipsadidae). *Zootaxa*, 3860, 64–80.
- Arteaga, A., Mebert, K., Valencia, J. H., Cisneros-Heredia, D. F., Peñafiel, N., Reyes-Puig, C., ... Guayasamin, J. M. (2017). Molecular phylogeny of *Atractus* (Serpentes, Dipsadidae), with emphasis on Ecuadorian species and the description of three new taxa. *ZooKeys*, 661, 91–123.
- Ávila-Pires, T. C. S. (2005). Reptiles. In T. Hollowell & R. P. Reynolds (Eds.), *Checklist of the Terrestrial Vertebrates of*

- the Guiana Shield (pp. 25–40). Washington, DC: Biological Society of Washington.
- Ávila-Pires, T. C. S., Hoogmoed, M. S., & Vitt, L. J. (2007). Herpetofauna da Amazônia. In L. B. Nascimento & M. E. Oliveira (Eds.), *Herpetologia no Brasil II* (pp. 13–43). Belo Horizonte: Sociedade Brasileira de Herpetologia.
- Ávila-Pires, T. C. S., Hoogmoed, M. S., & Rocha, W. A. (2010). Notes on the Vertebrates of northern Pará, Brazil: A forgotten part of the Guianan Region, I. Herpetofauna. *Boletim Do Museu Paraense Emílio Goeldi. Ciências Naturais*, 5, 113–112.
- Blair, C., Mendez de la Cruz, F. R., Ngo, A., Lindell, J., Lathrop, A., & Murphy, R. W. (2009). Molecular phylogenetics and taxonomy of leaf-toed geckos (Phyllodactylidae: *Phyllodactylus*) inhabiting the peninsula of Baja California. *Zootaxa*, 2027, 28–42.
- Bickham, J. W., Wood, C. C., & Patton, J. C. (1995). Biogeographic implications of cytochrome-b sequences and allozymes in sockeye (*Oncorhynchus nerka*). *Journal of Heredity*, 86, 140–144.
- Boie, F. (1827). Bemerkungen Über Merrem's Verfuch eines Systema der Amphibien. *Isis Von Oken*, 20, 508–565.
- Boulenger, G. A. (1894). *Catalogue of the Snakes in the British Museum (Natural History)*. Vol. 2. London: Trustees of the British Museum.
- Chippaux, J. P. (1986). *Les serpents de la Guyane Française*. Paris: Ostrom.
- Cole, C. J., Townsend, C. R., Reynolds, R. P., MacCulloch, R. D., & Lathrop, A. (2013). Amphibians and reptiles of Guyana, South America: Illustrated keys, annotated species accounts, and a biogeographic synopsis. *Proceedings of the Biological Society of Washington*, 125, 317–578.
- Cunha, O. R., & Nascimento, F. P. (1978). Ofídios da Amazônia X: As cobras da região leste do Pará. *Publicações Avulsas Do Museu Paraense Emílio Goeldi*, 31, 1–218.
- Cunha, O. R., & Nascimento, F. P. (1983). Ofídios da Amazônia XX – As espécies de *Atractus* Wagler, 1828, na Amazônia oriental e Maranhão (Ophidia, Colubridae). *Boletim Do Museu Paraense Emílio Goeldi, Nova Série Zoologia*, 123, 1–38.
- Cunha, O. R., & Nascimento, F. P. (1984). Ofídios da Amazônia XXI – *Atractus zidoki* no leste do Pará e notas sobre *A. alphonsehoguei* e *A. schach*. *Boletim Do Museu Paraense Emílio Goeldi, Série Zoologia*, 1, 219–228.
- Cunha, O. R., & Nascimento, F. P. (1993). Ofídios da Amazônia X - As cobras da região Leste do Pará. *Boletim Do Museu Paraense Emílio Goeldi*, 9, 1–191.
- Dowling, H. G. (1951). A proposed standard system of counting ventrals in snakes. *British Journal of Herpetology*, 1, 97–99.
- Dowling, H. G., & Savage, J. M. (1960). A guide to snake hemipenis: a survey of basic structure and systematic characteristics. *Zoologica*, 45, 17–28.
- Drummond, A. J., Suchard, M. A., Xie, D., & Rambaut, A. (2012). Bayesian phylogenetics with BEAUti and the BEAST 1.7. *Molecular Biology and Evolution*, 29, 1969–1973.
- Duméril, A. M. C., Bibron, G., & Duméril, A. H. A. (1854). *Erpétologie Générale ou Histoire Naturelle Complète des Reptiles*. Vol. 7. Paris: Librairie Encyclopédique de Roret.
- Figuroa, A., McKelvy, A. D., Grismer, L. L., Bell, C. D., & Lailvaux, S. P. (2016). A species-level phylogeny of extant snakes with description of a new colubrid subfamily and genus. *Public Library of Science One*, 11, 1–31.
- Fouquet, A., Gilles, A., Vences, M., & Marty, C. (2007). Underestimation of species richness in Neotropical frogs revealed by mtDNA analyses. *Public Library of Science One*, 2, e1109.
- Fouquet, A., Vacher, J.-P., Courtois, E. A., Villette, B., Reizine, H., Gaucher, P., ... Kok, P. J. R. (2018). On the brink of extinction: two new species of *Anomaloglossus* from French Guiana and amended definitions of *Anomaloglossus degranvillei* and *A. surinamensis* (Anura: Aromobatidae). *Zootaxa*, 4379, 1–23.
- Fraga, R., Lima, A. P., Prudente, A. L. C., & Magnusson, W. E. (2013). *Guia de cobras da região de Manaus – Amazônia Central*. Manaus: INPA.
- Fraga, R., Almeida, A. P., Moraes, L. C. J., Gordo, M., Pirani, R., Zamora, R. R., ... Werneck, F. P. (2017). Narrow endemism or insufficient sampling? Geographic range extension and morphological variation of the poorly known *Atractus riveroi* Roze, 1961 (Serpentes: Dipsadidae). *Herpetological Review*, 48, 281–284.
- Funk, W. C., Caminer, M., & Ron, S. R. (2012). High levels of cryptic species diversity uncovered in Amazonian frogs. *Proceedings of the Royal Society B*, 279, 1806–1814.
- Grazziotin, F. G., Zaher, H., Murphy, R. W., Scrocchi, G., Benavides, M. A., Zhang, Y. P., & Bonatto, S. L. (2012). Molecular phylogeny of the New World Dipsadidae (Serpentes: Colubroidea): a reappraisal. *Cladistics*, 28, 437–459.
- Hammond, D. S. (2005). *Tropical Forests of the Guiana Shield: Ancient Forests in a Modern World*. Wallingford: CABI Publishing.
- Hoegg, S., Vences, M., Brinkmann, H., & Meyer, A. (2004). Phylogeny and comparative substitution rates of frogs inferred from sequences of three nuclear genes. *Molecular Biology and Evolution*, 21, 1188–1200.
- Hoogmoed, M. S. (1979). The herpetofauna of the Guianan Region. In W. E. Duellman (Ed.), *The South American herpetofauna: its origin, evolution and dispersal* (pp. 241–279). Lawrence: The University of Kansas Monographs.
- Hoogmoed, M. S. (1980). Revision of the genus *Atractus* in Surinam, with the resurrection of two species (Colubridae, Reptilia). Notes on the Herpetofauna of Surinam VII. *Zoologische Verhandelingen*, 175, 1–47.
- Hoogmoed, M. S., & Ávila-Pires, T. C. S. (1991). Annotated checklist of the herpetofauna of Petit Saut, Sinnamary River, French Guiana. *Zoologische Mededelingen*, 65, 53–88.
- Hoogmoed, M. S., Pinto, R. R., Rocha, W. A., & Pereira, E. G. (2009). A new species of *Mesobaena* Mertens, 1925 (Squamata: Amphisbaenidae) from Brazilian Guiana, with a key to the Amphisbaenidae of the Guianan Region. *Herpetologica*, 65, 436–448.
- Hollowell, T., & Reynolds, R. P. (2005). Checklist of the terrestrial vertebrates of the Guiana Shield. *Bulletin of the Biological Society of Washington*, 13, 1–98.
- Kendall, S., Yeo, M., Henttu, P., & Tomlinson, D. R. (2001). Alternative splicing of the Neurotrophin-3 gene gives rise to different transcripts in a number of human and rat tissues. *Journal of Neurochemistry*, 75, 41–47.
- Kok, P. J. R. (2010). A new species of *Chironius* Fitzinger, 1826 (Squamata: Colubridae) from the Pantepui region, northeastern South America. *Zootaxa*, 2611, 31–44.
- Köhler, G. (2012). *Color catalogue for field biologists*. Affenbach: Herpeton.

- Kumar, S., Stecher, G., & Tamura, K. (2016). MEGA7: Molecular Evolutionary Genetics Analysis version 7.0 for bigger datasets. *Molecular Biology and Evolution*, 33, 1870–1874.
- Lanfear, R., Calcott, B., Ho, S. Y., & Guindon, S. (2012). PartitionFinder: combined selection of partitioning schemes and substitution models for phylogenetic analyses. *Molecular Biology and Evolution*, 29, 1695–1701.
- Lanfear, R., Frandsen, P. B., Wright, A. M., Senfeld, T., & Calcott, B. (2016). PartitionFinder 2: new methods for selecting partitioned models of evolution for molecular and morphological phylogenetic analyses. *Molecular Biology and Evolution*, 34, 772–773.
- Lawson, R., Slowinski, J. B., Crother, B. I., & Burbrink, F. T. (2005). Phylogeny of the Colubroidea (Serpentes): new evidence from mitochondrial and nuclear genes. *Molecular Phylogenetics and Evolution*, 37, 581–601.
- Martins, M., & Oliveira, M. E. (1993). The snakes of the genus *Atractus* Wagler (Reptilia: Squamata: Colubridae) from the Manaus region, central Amazônia, Brazil. *Zoologische Mededelingen*, 69, 21–40.
- Martins, M., & Oliveira, M. E. (1998). Natural history of snakes in forests of the Manaus region, central Amazonia, Brazil. *Herpetological Natural History*, 6, 78–150.
- Miller, M. A., Pfeiffer, W., & Schwartz, T. (2010). *Creating the CIPRES Science Gateway for inference of large phylogenetic trees*. Los Angeles: Proceedings of the Gateway Computing Environments Workshop.
- Moraes, L., Almeida, A., de Fraga, R., Zamora, R., Pirani, R., Silva, A., ... Werneck, F. (2017). Integrative overview of the herpetofauna from Serra da Mocidade, a granitic mountain range in northern Brazil. *ZooKeys*, 715, 103–159.
- Morato, S. A. A., Calixto, P. O., Mendes, L. R., Gomes, R., Galatti, U., Trein, F. L., ... Ferreira, G. N. (2014). *Guia fotográfico de identificação da herpetofauna da Floresta Nacional de Saracá-Taquera, Estado do Pará*. Curitiba: STCP Engenharia de Projetos Ltda.
- Morato, S.A.A., Ferreira, G.N., Scupino, M. R. C. Eds. (2018). *Herpetofauna da Amazônia Central: Estudos na FLONA de Saracá-Taquera*. Curitiba: STCP Engenharia de Projetos Ltda.
- Morrone, J. J. (2014). Biogeographical regionalisation of the Neotropical region. *Zootaxa*, 3782, 1–110.
- Murphy, J. C., Jowers, M. J., Lehtinen, R. M., Charles, S. P., Colli, G. R., Peres, A. K., ... Pyron, R. A. (2016). Cryptic, sympatric diversity in tegu lizards of the *Tupinambis teguixin* Group (Squamata, Sauria, Teiidae) and the description of three new species. *Plos One*, 11, e0158542.
- Nascimento, F. P., Ávila-Pires, T. C., & Cunha, O. R. (1988). Répteis Squamata de Rondônia e Mato Grosso coletados através do Programa Pólo Noroeste. *Boletim Do Museu Paraense Emílio Goeldi*, 4, 21–66.
- Oliveira, E. A., & Hernández-Ruz, E. J. (2016). Morphological variation in *Atractus tartarus* (Serpentes: Dipsadidae) from the Xingu River, east Amazon, Brazil and preliminary phylogenetic relationship in *Atractus*. *International Journal of Research Studies in Biosciences*, 4, 1–7.
- Padial, J. M., Castroviejo-Fisher, S., Köhler, J., Vilà, C., Chaparro, J. C., & De la Riva, I. (2009). Deciphering the products of evolution at the species level: the need for an integrative taxonomy. *Zoologica Scripta*, 38, 431–447.
- Palumbi, S. R., Martin, A., Romano, S., McMillan, W. O., Stice, L., & Grabowski, G. (1991). *The simple fool's guide to PCR, version 2*. Honolulu: University of Hawaii Zoology Department.
- Passos, P., Fernandes, D. S., & Borges-Nojosa, D. M. (2007). A new species of *Atractus* (Serpentes: Dipsadinae) from a relictual forest in northeastern Brazil. *Copeia*, 2007, 788–797.
- Passos, P., Lynch, J. D., & Fernandes, R. (2008). Taxonomic status of *Atractus sanctaemartae* and *Atractus nebularis*, and description of a new *Atractus* from the Atlantic coast of Colombia. *Herpetological Journal*, 18, 175–186.
- Passos, P., Rivas, G. F., & Barrio-Amorós, C. L. (2009). Description of two new species from Venezuela in the highly diverse dipsadine genus *Atractus* (Serpentes: Colubridae). *Amphibia-Reptilia*, 30, 233–243.
- Passos, P., Fernandes, R., Bérnils, R. S., & Moura-Leite, J. C. (2010). Taxonomic revision of Atlantic Forest *Atractus* (Serpentes: Dipsadidae). *Zootaxa*, 2364, 1–63.
- Passos, P., Cisneros-Heredia, D. F., Rivera, D. E., Aguilar, C., & Schargel, W. E. (2012). Rediscovery of *Atractus microrhynchus* and reappraisal of the taxonomic status of *A. emersoni* and *A. natans* (Serpentes: Dipsadidae). *Herpetologica*, 68, 375–392.
- Passos, P., & Prudente, A. L. C. (2012). Morphological variation, polymorphism and taxonomy of the *Atractus torquatus*3 complex (Serpentes: Dipsadidae). *Zootaxa*, 3407, 1–21.
- Passos, P., Kok, P. J. R., Albuquerque, N. R., & Rivas, G. (2013). Groundsnakes of the Lost World: a review of *Atractus* (Serpentes: Dipsadidae) from the Pantepui region, northern South America. *Herpetological Monographs*, 27, 52–86.
- Passos, P., Teixeira, M., Jr., Recoder, R., Sena, M. A., Dal Vechio, F., Pinto, ..., Rodrigues, M. T. (2013). A new species of *Atractus* (Serpentes: Dipsadidae) from Serra do Cipó, Espinhaço Range, Southeastern Brazil, with proposition of a new species group to the genus. *Papéis Avulsos de Zoologia*, 53, 75–85.
- Passos, P., Prudente, A. L. C., & Lynch, J. D. (2016). Redescription of *Atractus punctiventris* and description of two new *Atractus* (Serpentes: Dipsadidae) from Brazilian Amazonia. *Herpetological Monographs*, 30, 1–20.
- Passos, P., Ramos, L. O., Fouquet, A., & Prudente, A. L. C. (2017). Taxonomy, morphology and distribution of *Atractus flammigerus* Boie, 1827 (Serpentes: Dipsadidae). *Herpetologica*, 73, 349–363.
- Passos, P., Prudente, A. L. C., Ramos, L. O., Caicedo-Portilla, J. R., & Lynch, J. D. (2018). Species delimitations in the *Atractus collaris* complex (Serpentes: Dipsadidae). *Zootaxa*, 4392, 491–520.
- Pesantes, O. (1994). A method for preparing hemipenis of preserved snakes. *Journal of Herpetology*, 28, 93–95.
- Peters, J. A. (1964). *Dictionary of Herpetology*. New York: Hafner.
- Prudente, A. L. C., & Passos, P. (2008). A new species of *Atractus* Wagler, 1828 (Serpentes: Dipsadinae) from Guyana Plateau in Northern Brazil. *Journal of Herpetology*, 42, 723–732.
- Prudente, A. L. C., & Passos, P. (2010). New cryptic species of *Atractus* (Serpentes: Dipsadidae) from Brazilian Amazonia. *Copeia*, 2010, 397–404.
- Pyron, R. A., Burbrink, F. T., & Wiens, J. J. (2013). A phylogeny and revised classification of Squamata, including 4161 species of lizards and snakes. *BioMed Central Evolutionary Biology*, 13, 1–53.
- Pyron, R. A., Guayasamin, J. M., Peñafiel, N., Bustamante, L., & Arteaga, A. (2015). Systematics of Nothopsini

- (Serpentes, Dipsadidae), with a new species of *Synophis* from the Pacific Andean slopes of southwestern Ecuador. *ZooKeys*, 541, 109–147.
- Pyron, R. A., Arteaga, A., Echevarría, L. Y., & Torres-Carvajal, O. (2016). A revision and key for the tribe Diaphorolepidini (Serpentes: Dipsadidae) and checklist for the genus *Synophis*. *Zootaxa*, 4171, 293–320.
- Ribeiro, M. A., Jr, Silva, M. B., & Lima, J. D. (2016). A new species of *Bachia* Gray 1845 (Squamata: Gymnophthalmidae) from the Eastern Guiana Shield. *Herpetologica*, 72, 148–156.
- Ronquist, F., Teslenko, M., van der Mark, P., Ayres, D. L., Darling, A., Höhna, S., ... Huelsenbeck, J. P. (2012). MrBayes 3.2: efficient Bayesian phylogenetic inference and model choice across a large model space. *Systematic Biology*, 61, 539–542.
- Sabaj, M. H. (2016). *Standard symbolic codes for institutional resource collections in herpetology and ichthyology: an online reference*. Version 6.5. Washington, DC: American Society of Ichthyologists and Herpetologists. Retrieved from <http://www.asih.org/> (accessed 16 August 2016).
- Savage, J. M. (1960). A revision of the Ecuadorian snakes of the colubrid genus *Atractus*. *Miscellaneous Publications of the Museum of Zoology University of Michigan*, 112, 1–86.
- Schargel, W., Lamar, W. W., Passos, P., Valencia, J. H., Cisneros-Heredia, D. F., & Campbell, J. A. (2013). A new giant *Atractus* (Serpentes: Dipsadidae) from Ecuador, with notes on some other large Amazonian congeners. *Zootaxa*, 3721, 455–474.
- Schlegel, H. (1837). *Essai sur la physionomie des serpens*. Vol. 1 and 2. Amsterdam: La Haye (J. Kips, J. HZ. et W. P. van Stockum).
- Starace, F. (1998). *Guide de serpents et amphibènes de Guyane*. Gadeloupe: Ibis Rouge.
- Sullivan, J., & Joyce, P. (2005). Model selection in phylogenetics. *Annual Review of Ecology, Evolution, and Systematics*, 36, 445–466.
- Thompson, J. D., Higgins, D. G., & Gibson, T. J. (1994). CLUSTAL W: improving the sensitivity of progressive multiple sequence alignment through sequence weighting, position-specific gap penalties and weight matrix choice. *Nucleic Acids Research*, 22, 4673–4680.
- Torres-Carvajal, O., Lobos, S. E., & Venegas, P. J. (2015). Phylogeny of Neotropical *Cercosaura* (Squamata: Gymnophthalmidae) lizards. *Molecular Phylogenetics and Evolution*, 93, 281–288.
- Torres-Carvajal, O., Koch, C., Venegas, P. J., & Poe, S. (2017). Phylogeny and diversity of neotropical monkey lizards (Iguanidae: *Polychrus* Cuvier, 1817). *Public Library of Science One*, 12, e0178139.
- Vacher, J.-P., Kok, P. J. R., Rodrigues, M. T., Lima, J. D., Lorenzini, A., Martinez, Q., ... Fouquet, A. (2017). Cryptic diversity in Amazonian frogs: integrative taxonomy of the genus *Anomaloglossus* (Amphibia: Anura: Aromobatidae) reveals a unique case of diversification within the Guiana Shield. *Molecular Phylogenetics and Evolution*, 112, 158–173.
- Vaidya, G., Lohman, D. J., & Meier, R. (2011). SequenceMatrix: concatenation software for the fast assembly of multi-gene datasets with character set and codon information. *Cladistics*, 27, 171–180.
- van Lidth de Jeude, T. W. (1904). Reptiles and batrachians from Surinam. *Notes from the Leyden Museum*, 25, 83–94.
- Vidal, N., Kindl, S. G., Wong, A., & Hedges, S. B. (2000). Phylogenetic relationships of Xenodontine snakes inferred from 12S and 16S ribosomal RNA sequences. *Molecular Phylogenetics and Evolution*, 14, 389–402.
- Wagler, J. (1828). Auszüge aus seinem Systema Amphibiorum. *Isis Von Oken*, 21, 740–744.
- Wagler, J. G. (1830). *Natürliches System der Amphibien, mit vorangehender Classification der Saugthiere und Vogel. Ein Beitrag zur vergleichenden Zoologie*. München: J.G. Cotta schen Buchhandlung.
- Wilson, E. O. (1985). The biological diversity crisis. *Bioscience*, 35, 700–706.
- Zaher, H. (1999). Hemipenial morphology of the South American xenodontine snakes, with a proposal for a monophyletic Xenodontinae and a reappraisal of Colubroid hemipenes. *Bulletin of the American Museum of Natural History*, 240, 1–168.
- Zaher, H., Oliveira, M. E., & Franco, F. L. (2008). A new, brightly colored species of *Pseudoboa* Schneider, 1801 from the Amazon Basin (Serpentes, Xenodontinae). *Zootaxa*, 1674, 27–37.
- Zimmerman, B. L., & Rodrigues, M. T. (1990). Frogs, snakes, and lizards of the INPA-WWF Reserves near Manaus, Brazil. In A. H. Gentry (Ed.), *Four neotropical rainforests* (pp. 426–454). New Haven, CT: Yale University.

Associate Editor: Mark Wilkinson